REVIEWS OF MODERN PHYSICS VOLUME 41, NUMBER 1 JANUARY 1969

Shapes of Inhomogeneously Broadened Resonance Lines in Solids

A. M. STONEHAM
Theoretical Physics Division, Atomic Energy Research Establishment, Harwell, Berkshire, England

Inhomogeneous broadening has been observed in resonance lines in solids over the wide range of energies spanned by nuclear magnetic resonance, electron spin resonance, optical, and Mössbauer methods. The broadening arises from random strains, electric fields, and other perturbations from the defects in the lattice containing the centre whose transitions are studied. This paper reviews the calculation of the shapes of such resonance lines. The most important method used is the so-called statistical method. This method determines the line shape as a function of the distribution of the defects with respect to the centres studied, the density of the defects, and the perturbation fields of the individual defects. Emphasis is laid on the physical assumptions and approximations in this method and on its relation to other approaches. The theory is applied to a variety of broadening mechanisms, both in the widely used continuum approximation for the lattice containing the defects and in the more realistic discrete-lattice model. Two classes of experimental work are reviewed. The first deals with the ways in which resonance lines are recognised as being inhomogeneously broadened. These methods show that a wide range of phenomena can be used to check the theory of the line shapes. The second discussion of the experimental work compares theory and experiment for each of the various broadening mechanisms. These mechanisms include broadening by the strains from dislocations and point defects, by the electric fields and field gradients from charged defects, and by unresolved hyperfine structure. In each case theory and experiment are compared in detail for the system for which the most complete data are available. The conclusion is that the statistical method provides a satisfactory approach in all cases for which there are adequate data.

CONTENTS

1. INTRODUCTION

Defects in solids give rise to sharp absorption lines over a very wide range of energies. These are seen in nuclear magnetic resonance (NMR) ($\sim 10^{-8}$ eV), electron spin resonance (EPR) ($\sim 10^{-4}$ eV), optical absorption (0.1–10 eV), and using the Mössbauer effect (usually 14.4 keV) with an over-all range of 10^{12} in energy. These lines give information about both the static and dynamic features of the environment of the defect. Further, for sharp lines, low integrated intensities can be measured, so that weakly allowed transitions and strong transitions from rare defects can both be observed.

The transitions differ widely in nature. Thus, the optical lines are essentially electronic phenomena, whereas the Mössbauer transitions are nuclear in origin. The factors which determine the *shapes* of the lines are, however, very similar in all cases, and a number of broadening mechanisms are common to the various transitions. The theory of the line shapes reflects this unity in that calculations are based on a small number of rather general methods which emphasise the points of similarity. For example, much of this review uses the "statistical method." This method has been used in the literature in many special cases,[1–21] although it has not always been emphasised that there were special cases of a method of great generality and wide application. Such points will be stressed in the present review, and the ground common to all branches of spectroscopy emphasised. We will also try to indicate any essential physical assumptions and the limits they impose. The broadening of a resonance line can be described by one of three labels. Extreme examples of *homogeneous* and *inhomogeneous* resonance lines[22] are illustrated in Fig. 1. A third class, *intermediate*, includes the inevitable borderline cases between the other two categories. The observed line is, of course, the superposition of the individual contributions. For homogeneous broadening,

all the centres responsible for the resonance line give contributions which have the same peak frequency and width. The most obvious case occurs when the linewidth is caused by the finite lifetimes of the states between which the transitions occur.[23] For inhomogeneous broadening the centres have a wide variety of peak frequencies. Their widths are usually similar but are appreciably less than the width of the distribution of peak frequencies. Examples of mechanisms giving inhomogeneous broadening are strain broadening (due to dislocations and point effects in the host lattice containing the centres), broadening due to the random electric fields and field gradients of charged defects, and the hyperfine interaction of the wavefunction of the centre with the nuclei of neighbouring ions. Intermediate cases are usually those in which several mechanisms give similar contributions to the broadening; some of these mechanisms favour inhomogeneity, others favour homogeneity. It should be emphasised, however, that the description of a line as homogeneous or inhomogeneous depends on the type of experiment involved. The usual criterion is "if the resonance line is excited in some narrow band of frequencies, are the other parts of the line affected appreciably in a time of the order of the characteristic time of the experiment"? A very clear illustration of this point comes from Wagner's study of the recovery of inverted spin systems.[24] In the "phonon avalanche" region[24a] the characteristic time is 10^{-5} sec and the line behaves inhomogeneously; in the "phonon bottleneck" regime the time constant is 10^{-2} sec and the line behaves homogeneously.

Three methods have proved particularly fruitful. Kubo and Tomita's work, based on the method of cumulants, has been especially valuable for homogeneous lines.[25,26] The method of moments has been widely used[27–29] and gives the moments

$$M_n = \int_{-\infty}^{\infty} d\omega \omega^n I(\omega) \Big/ \int_{-\infty}^{\infty} d\omega I(\omega)$$

of the line shape $I(\omega)$, rather than the line shape itself. Although the moment method gives a number of elegant exact results, these results are often misleading if the qualitative features of the line shape are not clearly understood.[28] The third method, on which this review will concentrate, is the statistical method (or Markoff method). It has proved useful in the theory of inhomogeneously broadened resonance lines and continues to be useful even when homogeneous broadening also occurs. Later the detailed relationships of these approaches will be examined. The three methods do not, of course, exhaust the possible approaches (for example, a separate treatment is needed to deal with the effects of mosaic structure[30]) but are sufficient to treat all the problems of the shapes of the resonance lines of centres in single crystals.

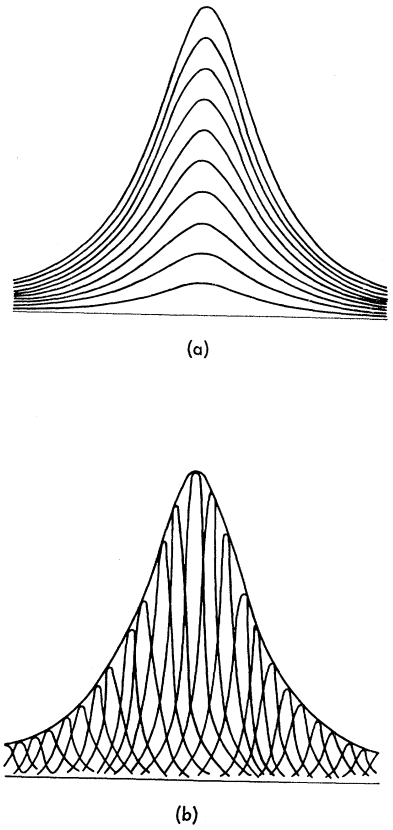

FIG. 1. Schematic diagram showing the two extreme classes of broadening. (a) Homogeneous broadening; (b) inhomogeneous broadening.

Inhomogeneous broadening is common to all branches of solid-state spectroscopy. Other mechanisms of line broadening are important in more restricted fields. For completeness, we briefly describe the most important of these mechanisms and indicate some recent articles which review them in detail.

The other types of broadening fit into two major classes: the interaction with collective excitations, such as phonons or magnons, and the interaction between the centres responsible for the resonance line. The interaction with collective excitations takes two main forms; both become more important at high temperatures. First, if the transition energy is much larger than the typical collective excitation energy, the transition will be accompanied by the absorption and emission of quanta of the excitation. Thus, in the optical absorption of the F centre in alkali halides, large numbers of phonons are emitted. This type of line broadening is discussed in Ref. 30(a). Second, the lifetimes of the states involved in a transition may be determined by the interaction of the centre involved with collective excitations. In spin resonance, for instance, spin–lattice relaxation may broaden the resonance line; it is then

the rate of exchange of energy between the spins and the phonons which is important. Such cases are discussed in Ref. 30(b). Finally, the interaction between centres is particularly important in spin resonance, where dipolar and exchange interactions affect the line shape. These phenomena are discussed in Ref. 30(c).

Three main questions are considered in this review. The first is, "How does one distinguish between homogeneous and inhomogeneous lines experimentally?" This question is treated in Sec. 2, where the methods which have proved useful are outlined with emphasis on the qualitative features of the experiments. The second question deals with the calculation of the line shapes of inhomogeneous lines in terms of the distribution of the defects responsible for the broadening. The statistical method and the physical assumptions implicit in its use are given in Sec. 3. Its detailed application is given in two degrees of sophistication in Secs. 4 and 5. In Sec. 4 the host lattice is treated as an isotropic homogeneous continuum. The simplicity is removed in Sec. 5, where the lattice structure is taken into account directly. The final question concerns the agreement between theory and experiment. This can only be answered in a small number of cases, as one must know both the inhomogeneous line shape and the nature and distribution of the defects responsible for the broadening. Such cases are described in Sec. 6.

2. THE IDENTIFICATION OF INHOMOGENEOUSLY BROADENED LINES

Certain experiments identify a particular resonance line as inhomogeneously broadened. These experiments suggest features which can be compared with theory and most give some quantitative results, although the data which can be extracted from them will not be analysed in detail until Sec. 6. Most of the important methods will be discussed, but not every paper which has used them will be mentioned.

Most of the methods are specific to one class of resonance lines alone; for example, they may only apply to spin-resonance lines. Two techniques, however, can be applied to all classes of resonance line, at least in principle: varying the number of defects, and comparing the effects of defects on different resonance lines.

The first general method is to change the concentration of the defects causing the broadening while keeping other factors constant. Thus, Bloembergen and Rowland[31] observed that dislocations produced in hard-working copper broadened the satellites observed in the nuclear magnetic resonance of ^{63}Cu and that annealing tended to restore the lines. Reif[32] found a variation in the intensities of the ^{79}Br and ^{81}Br resonances in AgBr on adding Cd^{2+} and on the creation of intrinsic defects by heating. Similarly, defects are removed on annealing radiation-damaged crystals, and annealing is often essential to getting reasonably sharp zero-phonon lines.[33] The extent of the inhomogeneous broadening can be estimated for both the original and final lines from the change in linewidth.

The second technique with wide application is to compare the widths and shapes of a number of lines in any one specimen and to see if these are consistent with the same distribution of microscopic strains or fields. This method is particularly common in spin resonance. Thus, McMahon[34] was able to compare the line shapes of the $\Delta M=1$, $\Delta M=2$, and double-quantum transitions in the EPR of $MgO:Fe^{2+}$. Feher[35] compared the linewidths of Fe^{3+} and Mn^{2+} in MgO and their variation with magnetic-field orientation. The ENDOR linewidth and the variation of EPR linewidth with hyperfine line for $MgO:Co^{2+}$ are consistent with strain broadening.[36] Schawlow's comparison[37] of the EPR and optical R linewidths of Cr^{3+} in ruby also suggests that the lines are strain broadened. Again, strain broadening has been identified recently in the antiferromagnetic resonance of $RbMnF_3$.[38] Here the crystal changes under stress from a state in which the magneto-elastic anisotropy is dominant to one in which the intrinsic cubic anisotropy dominates. In each region the observed transition energy is linear in the strain, but the coupling coefficients are different. The linewidths are consistent with the assumption that the distribution of strains is the same in both cases.

The approach of comparing different lines in the same crystal is open to a number of dangers. First, if the lines considered come from different species of centre, there is the possibility that one of these centres is strongly correlated with the defects which broaden the lines. The comparison will then suggest that different mechanisms are responsible for broadening in the two cases. Second, the widths of the lines concerned may have contributions from several mechanisms, and allowance must be made for all of them. As an example, in comparing spin resonance and optical lines one must allow for dipolar broadening of the EPR line and for the broadening of the optical line from the interaction of the centre with phonons. Third, it must be recognised that the combination of strain or electric-field components which appears in the transition energy will differ for various transitions. If the transition energy is related to the strain tensor $\mathbf{e}$ by

$$\hbar\omega=\hbar\omega_0+\hbar\omega_1\sum_{i,j}a_{ij}e_{ij}, \tag{2.1}$$

then the a_{ij} for optical transitions need not be proportional to those for EPR transitions. In fact, the EPR coefficients vary with the direction of the magnetic field. Thus, different transitions sample different components of $\mathbf{e}$ and may give different shapes and widths a simple comparison of the widths is possible only to order of magnitude.

In addition to these general methods there are others with restricted application; these apply to EPR transi-

tions almost exclusively. The first utilizes the fact that the defects causing broadening are usually quite different from those whose resonance is studied. Thus, the inhomogeneous width will be independent of the spin concentration, unlike the case of the dipolar contribution.[14,39] This is the case for MgO:Fe^{2+} (Ref. 34) and is, in fact, seen for low concentrations of most transition-metal ions in MgO. The second group of methods takes advantage of the fact that only a small fraction of the spins contribute to a given part of the resonance line. The line can then be saturated in a narrow region using one microwave signal ("burning a hole" in the line) while the saturation is observed with another signal. This has been done at microwave frequencies with conventional EPR[40b] by saturating with microwave phonons[40b] and also optically.[41] The third set of methods recognises that the variation of linewidth with magnetic field and hyperfine line is different for inhomogeneous lines. For simplicity we illustrate this for spins of $S=\frac{1}{2}$ with an isotropic g factor and hyperfine interaction. The unperturbed transition energy is

$$\hbar\omega_0=g\beta H+AI_z; \tag{2.2}$$

second-order terms are omitted. Under a strain $d\epsilon$ the energy is changed by

$$\hbar(\omega-\omega_0)=[(\partial g/\partial\epsilon)\beta H+(\partial A/\partial\epsilon)I_z]\,d\epsilon. \tag{2.3}$$

If the strain distribution in the crystal has width $\epsilon_{1/2}$, the observed width of the resonance line will be

$$(\partial g/\partial\epsilon)\epsilon_{1/2}\beta H+(\partial A/\partial\epsilon)\epsilon_{1/2}I_z. \tag{2.4}$$

Clearly for a species with no nuclear spin ($I=0$), the width is proportional to the magnetic field. With pure dipolar broadening the width is independent of H, as shown by van Vleck's moment results.[27] If I is finite, the width varies with the hyperfine line because of the term in I_z. The variation with I_z and H has been seen for MgO:Co^{2+}.[36,42] For systems with spin greater than $\frac{1}{2}$, Eqs. (2.2)–(2.4) contain additional terms which lead to a dependence of the $S_z\rightarrow S_z+1$ transition on S_z. For non-Kramers ions, inhomogeneous effects can split levels which are degenerate when unperturbed and in a zero magnetic field; this can lead to enhanced absorption in zero magnetic field.

Fourth, Portis[43] has shown that inhomogeneous lines can be recognised by their saturation behavior. As the saturating power is raised, the absorption signal should saturate (i.e., tend to a finite limit), whereas the dispersion should be proportional to the square root of the power. This has been observed in the EPR of the F centre (Ref. 44 and references therein) and in paraelectric resonance.[45] Finally there is a suggestive technique based on an approximate result. Equation (2.1) relates the transition energy of one centre to the local strain. It can also be taken to relate the peak of the observed resonance line to an externally applied strain. As the direction of the magnetic field changes in an EPR experiment, the a_{ij}'s change, and as the local strains all remain constant, the linewidth changes. Usually one of the a_{ij} is of dominant importance; because of the particular form of the strain distribution and the magnitudes of the coupling coefficients, the corresponding e_{ij} is the most important strain component. The change in width with field orientation then reflects the variation of a_{ij}. If a static stress producing a strain which is predominantly e_{ij} is applied, then the variation in the position of the peak of the line will again reflect the variation of a_{ij}. Comparing the two experiments, the line shift under a static stress and the linewidth should both vary in the same way as the magnetic-field orientation is altered. If the linewidth and the shift under stress do vary similarly, then strain broadening is suggested. Correspondingly, if the width and the shift under an external electric field vary similarly, broadening by random fields is suggested. The approximation occurs because the components of the local strain other than e_{ij} have been dropped; the difficulty of the method is that one must guess which e_{ij} to ignore. The method does not work equally well for all systems. The approach has been used for electric-field broadening[15] and strain broadening.[46]

Finally we note that dipolar or exchange narrowing may complicate the analysis of inhomogeneous broadening in magnetic-resonance lines.[47–49] This effect is important in ferromagnetic resonance and also in paramagnetic resonance when the perturbing field is small compared with the magnetisation. The linewidth then depends on the shape of the sample and decreases with the magnetisation.[49]

3. THE STATISTICAL METHOD

This method provides the most powerful approach in calculating inhomogeneous line shapes. This section treats the assumptions, limits, and results of the method itself and relates the method to other approaches.

3.1 The Range of Application of the Statistical Method

Here we review the physical assumptions made in applying the method to inhomogeneous broadening. These are the basic assumptions common to most cases, rather than the special expedient assumptions peculiar to individual problems. The basic assumptions will be illustrated by particular reference to broadening by random strains and by random electric fields.

The first assumption is that the transition energy is linear in the local strain, i.e.,

$$\hbar\omega=\hbar\omega_0+\hbar\omega_1\sum_{i,j}a_{ij}e_{ij}, \tag{3.1}$$

or the local electric field, i.e.,

$$\hbar\omega=\hbar\omega_0+\hbar\omega_1\sum_{i}\alpha_iE_i/E_0. \tag{3.2}$$

In these equations $\hbar\omega_1 a_{ij}$ and $\hbar\omega_1\alpha_i$ are coupling coefficients which can be measured in separate experiments in which the transition is observed under an externally applied stress[35,50] or electric field.[51] The relative values of the a_{ij} and α_i are determined largely by symmetry; this will be discussed again later. To simplify our notation we write (3.1) and (3.2) in a common form:

$$\hbar\omega=\hbar\omega_0+\hbar\omega_1\epsilon, \tag{3.3}$$

where

$$\epsilon=\sum_{i,j} a_{ij}e_{ij} \tag{3.4}$$

for strain broadening, and

$$\epsilon=\sum_i \alpha_i E_i/E_0 \tag{3.5}$$

for broadening by electric fields. The electric field E_0 is introduced to ensure that ϵ is dimensionless. The a_{ij} and α_i are also dimensionless and depend on the symmetry of the centre and the host lattice and on the direction of any applied field.

This assumption is essentially that of first-order perturbation theory and means that we may calculate the line shape (i.e., the distribution of $\hbar\omega$) by calculating the distribution of ϵ. We calculate directly the probability $I(\epsilon)\,d\epsilon$ that ϵ lies in the range ϵ to $\epsilon+d\epsilon$. The observed line shape is related by scaling, i.e.,

$$I_{\rm obs}[\hbar(\omega-\omega_0)]=I[\epsilon=(\omega-\omega_0)/\omega_1]. \tag{3.6}$$

The assumption can be generalised in a number of ways. The work can be extended to treat terms quadratic in the strain or field components. This extension is described later and is not trivial, largely because the second basic assumption (stated below) fails in this case. A second-order theory is needed for the $\Delta M=2$ and double-quantum lines in MgO:Fe^{2+}, for example.[34] A further useful generalisation treats transitions which split under stress. If the ith component has a transition energy

$$\hbar\omega_1=\hbar\omega_0+\hbar\omega_1\beta_i\epsilon \tag{3.7}$$

and a fraction $f_i(\epsilon)$ of the total intensity, then the intensity at frequency ω due to all the components is

$$I_{\rm obs}[\hbar(\omega-\omega_0)]=\sum f_i[(\omega-\omega_0)/\omega_1\beta_i]I[(\omega-\omega_0)/\omega_1\beta_i]. \tag{3.8}$$

This should be compared with (3.6); (3.8) applies to the rather large number of optical zero-phonon lines which split under stress.[52–54]

The second assumption is that the contributions to ϵ of all the defects* which cause broadening simply add linearly. If we define Z_i as a variable which gives the position $\mathbf{r}_i$ and any relevant internal variables η_i of the ith defect, the contributions to ϵ are then additive; i.e.,

$$\epsilon(Z_1, Z_2, \cdots, Z_N)=\sum_{i=1}^{N}\epsilon(Z_i). \tag{3.9}$$

For broadening by microscopic strains, this is the assumption of linear elasticity, i.e., we may ignore terms in the free-energy quadratic in the strains. Nonlinear effects usually become appreciable for strains greater than about 10^{-2}. As the half-widths of internal strain distributions are typically 10^{-4}, nonlinear terms should be negligible. We will, however, return to this point later. If the resonance line is broadened by microscopic electric fields, (3.9) is equivalent to the assumption that nonlinear effects are negligible. The terms in the dielectric constant which depend on the field become significant for electric fields of the order of 10^6–10^7 V/cm, which is considerably greater than the 10^5 V/cm typical of the widths of observed internal-field distributions.

The third and final assumption is that the defects which cause the broadening are not correlated with each other. In general, the probability of a specific configuration of the defects $\{Z_1, Z_2, \cdots, Z_N\}$ is a function of the positions and internal variables (given by Z_i) of all the N defects, $P(Z_1, \cdots, Z_N)\,dZ_1\cdots dZ_N$. Our assumption is that $P(Z_1, \cdots, Z_N)$ may be factorised in the form

$$P(Z_1, \cdots, Z_N)=p(Z_1)p(Z_2)\cdots p(Z_N). \tag{3.10}$$

This relation cannot be exact; the restriction that defects cannot occupy the same site means (3.10) is approximate, even in the absence of other interactions between the defects. Correspondingly, the assumption (3.10) is only good for low defect concentrations. In practice, for the most interesting cases, the defect concentrations rarely exceed 10^{-3} (0.1 at.%) and we might expect the approximation to be reasonable. At higher concentrations a more sophisticated theory is needed, possibly developing along the lines of Ref. 55.

3.2 The Statistical Method

This section outlines the statistical method in a form suitable for treating all the line-shape problems of interest. The assumptions outlined in Sec. 3.1 are adopted, so we assume the transition energy to be linear in the perturbation ϵ:

$$\hbar\omega=\hbar\omega_0+\hbar\omega_1\epsilon; \tag{3.3}$$

that the contributions of the various defects to ϵ are simply additive:

$$\epsilon(Z_1, \cdots, Z_N)=\sum_{i=1}\epsilon(Z_i); \tag{3.9}$$

and that the defects are uncorrelated in the sense that

* We will use the term "centre" to describe whatever gives rise to the resonance line. The word "defect" will be used for any imperfection which causes broadening of a resonance line. Thus, a particular species may be referred to as a "centre" in one context, when its own transitions are being studied, and as a "defect" elsewhere, when its effect on another species is being discussed. All other terms, such as "colour centre," will be used conventionally, and will not indicate the role played by the species.

the probability of a particular configuration can be written as

$$p(Z_1)\, dZ_1 \cdots p(Z_N)\, dZ_N. \tag{3.11}$$

We now calculate $I(\epsilon)\, d\epsilon$, the probability that ϵ lies in the range ϵ to $\epsilon+d\epsilon$, in terms of the perturbations of the individual defects $\epsilon(Z_i)$, and the statistical distribution of the defects, given by $p(Z_i)$.

Each configuration $\{Z_1, \cdots, Z_N\}$ corresponds to a specific arrangement of the N perturbing defects in which the positions $(\mathbf{r}_i)$ and the other parameters (η_i) which describe every one of the centres have definite values. The statistical assumptions about the probability distribution of each of the Z_i are contained in a statistical weight function $p(Z_i)$. If the centre whose transition is observed is at $\mathbf{R}$ then $p(Z_i)$ is the probability that the ith defect is at $\mathbf{R}+\mathbf{r}_i$ with internal variables given by η_i. Clearly $p(Z)$ is closely related to the pair distribution function of the position of the defects with respect to the centres whose transitions are studied. We normalise $p(Z)$ by

$$\int dZ p(Z) = v \tag{3.12}$$

and define the *density* of defects by

$$\rho \equiv N/v. \tag{3.13}$$

The explicit form of $p(Z)$ will be given later in a number of cases. We will assume, for simplicity, that there is only one type of defect. This assumption will be generalised subsequently.

The fraction of all the defect configurations which produce a given value of ϵ at the point of observation is

$$I(\epsilon) = v^{-N} \int dZ_1 p(Z_1) \cdots \times \int dZ_N p(Z_N)\, \delta[\epsilon - \epsilon(Z_1, \cdots, Z_N)]. \tag{3.14}$$

The delta function singles out the configurations for which $\epsilon(Z_1, \cdots, Z_N)$ has the value ϵ. For this reason, singularities in $\epsilon(Z_1, \cdots, Z_N)$ do not cause difficulties, as the configurations to which they correspond have been excluded. Such singularities are, however, very important in calculating the moments of $I(\epsilon)$ which are discussed in Sec. 3.3.

Equation (3.14) may be rewritten using the spectral representation of the delta function:

$$\delta(y) = \frac{1}{2\pi} \int_{-\infty}^{\infty} dx \exp(ixy), \tag{3.15}$$

giving

$$I(\epsilon) = v^{-N} \frac{1}{2\pi} \int_{-\infty}^{\infty} dx \int dZ_1 p(Z_1) \cdots \int dZ_N p(Z_N) \times \exp\{ix[\epsilon - \epsilon(Z_1, \cdots, Z_N)]\}. \tag{3.16}$$

The spectral variable x in this equation has no special physical significance. The contributions of the defects to ϵ add linearly, so (3.16) may be factorised using (3.9):

$$I(\epsilon) = \frac{1}{2\pi} \int_{-\infty}^{\infty} dx \exp(ix\epsilon) \times \left(v^{-1} \int dZ p(Z) \exp[-ix\epsilon(Z)] \right)^N. \tag{3.17}$$

We introduce a function $J(x)$ where

$$v^{-1} \int dz p(z) \exp[-ix\epsilon(z)] = 1 - v^{-1} J(x) = 1 - N^{-1} \rho J(x). \tag{3.18}$$

The density of defects ρ is given by (3.13). Thus,

$$J(x) = \int dz p(z) \{1 - \exp[-ix\epsilon(z)]\}. \tag{3.19}$$

Recalling that in the limit of large N, $(1-A/N)^N$ tends to $\exp(-A)$, we finally obtain

$$I(\epsilon) = \frac{1}{2\pi} \int_{-\infty}^{\infty} dx \exp(ix\epsilon) \exp[-\rho J(x)]. \tag{3.20}$$

This equation, together with the definitions (3.19) and (3.13), gives the distribution in magnitude of the perturbation ϵ in terms of the perturbation fields of the individual defects $\epsilon(z)$, the density of the defects ρ and their statistical distribution $p(z)$.

Our final result (3.20) can be simplified in one case, expecially useful in practice, where $I(\epsilon)$ is symmetric about $\epsilon=0$. Then $I(\epsilon)$ and $I(-\epsilon)$ are equal, and

$$I(\epsilon) = \pi^{-1} \int_0^{\infty} dx \cos(x\epsilon) \exp[-\rho J(x)], \tag{3.21}$$

$$J(x) = \int dz p(z) \{1 - \cos[x\epsilon(z)]\}. \tag{3.22}$$

3.3 Extensions of the Fundamental Results

The fundamental equations (3.13), (3.19), and (3.20) are sufficient to calculate line shapes in many cases of interest. It is convenient to extend these equations in several ways. Two which are useful approximations are the moment method and an approximate method which gives the linewidth directly. These are useful in broadening from unresolved hyperfine structure as the analytic results based on (3.20) are usually intractable or inappropriate. Two are straightforward extensions of Sec. 3.2 and treat the simultaneous broadening due to several species of defect and the distribution of the sum of the two components $\epsilon_1+\epsilon_2$; here it is shown that, as a general rule, the dipolar and inhomogeneous contributions to an EPR linewidth

should simply be convolved in predicting the line shape. Finally, we will consider second-order effects and calculate the distribution of the product of two components $\epsilon_1\epsilon_2$.

3.3.1 The Moments of the Line Shape

Theories of line shapes[27–29] often calculate the moments of the shape, defined by

$$M_n=\int_{-\infty}^{\infty} d\epsilon\epsilon^n I(\epsilon) \Big/ \int_{-\infty}^{\infty} d\epsilon I(\epsilon). \quad (3.23)$$

The moments are not measured directly in experiment; their one advantage is that they can be calculated without difficulty in some cases. Such calculations should be contrasted with our discussion in Sec. 3.2 in which the line shape $I(\epsilon)$ was found directly. The few advantages of calculating moments are usually lacking for inhomogeneously broadened lines. Indeed, as the moments are dominated by the regions where ϵ is large they are not even finite unless great care is taken.

The moments are best expressed in terms of integrals S_n where

$$S_n=\rho\int dzp(z)[\epsilon(z)]^n. \quad (3.24)$$

The S_n vanish for symmetric lines when n is odd; S_0 is equal to N by (3.12) and (3.13). The moments can be found by the method of Ref. 29, which is to expand the term $\exp(ix\epsilon)$ in (3.20) and then differentiate with respect to x. Thus,

$$M_n=\lim_{x\to 0}(-1)^n[d^n/d(ix)^n]\exp[-\rho J(x)] \quad (3.25)$$

which gives as the first few moments

$$\begin{aligned}
M_0&=1,\\
M_1&=S_1,\\
M_2&=S_2+S_1^2,\\
M_3&=S_3+3S_1S_2+S_1^3,\\
M_4&=S_4+4S_1S_3+3S_2^2+6S_2S_1^2+S_1^4\\
&=(S_4+4S_1S_3-2S_1^4)+3(M_2)^2. \quad (3.26)
\end{aligned}$$

In the case of symmetric lines there is some simplification:

$$\begin{aligned}
M_1&=0,\\
M_2&=S_2,\\
M_3&=0,\\
M_4&=S_4+3M_2^2. \quad (3.27)
\end{aligned}$$

For a Gaussian shape $M_4=3M_2^2$, which would require S_4 to be zero. This happens in rather unusual circumstances, so that whilst predicted shapes may be asymptotically Gaussian they are rarely exactly so.

3.3.2 Approximate Linewidths

The most important parameters measured experimentally are the peak height and linewidth. These can be obtained approximately without going through a complex calculation of $I(\epsilon)$ and subsequent analysis. The method[56] exploits the fact that, for a line of given width and peak height, the centre of the line (the part between the points of half intensity) is nearly the same for such extremes as the Gaussian shape, where $I(x)\sim\exp(-x^2/a^2)$, and the Lorentzian shape, for which $I(x)\sim 1/(x^2+a^2)$. The method fits a Lorentzian to the peak and the point of half-intensity and height of the fitted curve. Direct application of the method using (3.20) shows that the width Δ is given by the integral equation

$$\Delta^2=\rho\int dzp(z)[\epsilon(z)]^2F[\epsilon(z)/\Delta], \quad (3.28)$$

where

$$F(u)=2(u^2+6)/[(u^4+4)(u^2+1)],$$

and the peak intensity is given by

$$I(0)=\frac{e}{\pi\Delta}\exp\left[-2\rho\int dzp(z)\frac{\epsilon^2(z)}{\Delta^2+\epsilon^2(z)}\right]. \quad (3.29)$$

These results are exact for a Lorentz line shape. The integral equation is most easily solved graphically and offers considerable advantages in complicated cases, such as oscillating screened interactions, where

$$\epsilon(r)\sim[A\exp(-\alpha r)\cos\beta r]/r.$$

3.3.3 Several Types of Defect

In real crystals a number of distinct defects may broaden the resonance lines. For example, in radiation-damaged crystals both point defects and dislocations cause strain broadening. We assume that the statistical distribution of defects of species A is independent of the coordinates of the defects of species B, and vice versa. Thus the two species are not correlated. The discussion of Sec. 3.2 can be repeated with only minor changes. In particular (3.16) may be factorised to give (3.17) as before. Equation (3.20) still holds, but now $\rho J(x)$ is given by

$$\begin{aligned}
\rho J(x)=&\rho_A\int dzp_A(z)\{1-\exp[-ix\epsilon_A(z)]\}\\
&+\rho_B\int dzp_B(z)\{1-\exp[-ix\epsilon_B(z)]\} \quad (3.30)
\end{aligned}$$

for two species A and B. In this, $\rho_A=N_A/S\,dzp_A(z)$, and so on. The results (3.20) and (3.30) taken to-

gether mean that the line shape is simply the *convolution* of the line shape $I_A(\epsilon)$ when species A alone causes broadening, with the shape $I_B(\epsilon)$ when B alone broadens the line:

$$I(\epsilon)=\int_{-\infty}^{\infty} dsI_A(s)I_B(\epsilon-s). \tag{3.31}$$

3.3.4 The distribution of a Sum of Perturbations

In the detailed analysis of line shapes, it is convenient to assume that, for example, the distributions of two components of the strain tensor, e_{ij} and e_{kl}, are independent. If this were true, the distribution of the sum of these, $e_{ij}+e_{kl}$, would be given by straightforward convolution. In more general notation, if $I_i(\epsilon_i)$ is the distribution of ϵ_i and if $I_{12}(\epsilon_{12})$ gives the distribution of $\epsilon_{12}=\epsilon_1+\epsilon_2$, then we would have

$$I_{12}(\epsilon_{12})=\int_{-\infty}^{\infty} dtI_1(t)I_2(\epsilon_{12}-t). \tag{3.32}$$

It is straightforward to show that (3.32) is only valid if

$$\rho J_{12}(x)=\rho J_1(x)+\rho J_2(x) \tag{3.33}$$

in which

$$J_i(x)=\int dzp(z)\{1-\exp[-ix\epsilon_i(z)]\}.$$

However, (3.33) is only valid, in general, if ϵ_1 and ϵ_2 are produced by *different* defects. This can be seen intuitively as follows. When ϵ_1 is large, it suggests that one of the defects is close to the point of observation. If the defect also produces a component ϵ_2, ϵ_2 will probably also be large, so that ϵ_1 and ϵ_2 are correlated. As a specific example, in an isotropic crystal containing only screw dislocations the dilation vanishes everywhere, i.e.,

$$e_{xx}+e_{yy}+e_{zz}=0.$$

It would clearly be wrong to assume e_{xx}, e_{yy}, and e_{zz} independent. This equation is, of course, just a special case of the compatibility relations which must be satisfied by the strains.

Equations (3.32) and (3.33) hold in one case of practical importance, when magnetic-resonance lines are broadened by microscopic strains and by spin–spin interactions. The system MgO:Mn^{2+} (Ref. 35) and MgO:Co^{2+} (Refs. 36, 42) are examples of this. If the sources of strain are nonmagnetic and if the magnetic ions produce no strain, then ϵ_1 and ϵ_2 are produced by different imperfections, ϵ_1 from the strains and ϵ_2 from the spin–spin interaction. The line shape in this particularly simple case is the convolution of the shape due to spin–spin interactions alone with that due to strain broadening alone.

In cases where the two components are correlated, they may still be sufficiently independent for a routine analysis. If $\langle\epsilon_1\epsilon_2\rangle$, the average over all configurations of $\epsilon_1\epsilon_2$, is zero, then ϵ_1 and ϵ_2 are sufficiently independent for this purpose. By manipulating the moment formulae (3.23)–(3.26) or by the second-order discussion of Sec. 3.3.5 we can show

$$\langle\epsilon_1\epsilon_2\rangle=\rho\int dzp(z)\epsilon_1(z)\epsilon_2(z)$$
$$+\left(\rho\int dzp(z)\epsilon_1(z)\right)\left(\rho\int dup(u)\epsilon_2(u)\right). \tag{3.34}$$

The usefulness of this relation is that in certain cases (3.34) can be shown to be zero by symmetry arguments alone. For example, in several cases, such as broadening by dislocations,

$$\rho\int dzp(z)\epsilon_i(z)=0,$$

and the second term of (3.34) vanishes. Specialising to cubic crystals in which the $p(z)$ retains the cubic symmetry, we can *choose* ϵ_1 and ϵ_2 to make the first term of (3.34) vanish. This is done by selecting any two different members of the set $2e_{zz}-e_{xx}-e_{yy}$, $e_{xx}-e_{yy}$, $e_{xx}+e_{yy}+e_{zz}$, $e_{xy}+e_{yx}$, $e_{yz}+e_{zy}$, and $e_{zx}+e_{xz}$ as ϵ_1 and ϵ_2. In an analysis of the line shapes, it should be a reasonable approximation to treat ϵ_1 and ϵ_2 as independent. This is still an approximation, of course, as we have not shown higher-order correlations to be zero.

3.3.5 Second-Order Terms

Sometimes a transition energy does not shift linearly with the perturbation (say the local strain). These resonance lines usually show a shift quadratic in the perturbation

$$\hbar\omega=\hbar\omega_0+\hbar\omega_2\epsilon'\epsilon'', \tag{3.35}$$

where, in analogy with (3.4) and (3.5), $\epsilon'=\sum a_{ij}'e_{ij}$ and $\epsilon''=\sum_{ij} a_{ij}''e_{ij}$ are different linear combinations of strain components. An equation similar to (3.35) holds for the $\Delta M=2$ and double quantum lines in the spin resonance of MgO:Fe^{2+}.[34] In this section we attempt to find the distribution of

$$\Omega=\epsilon'\epsilon''=\sum_i \epsilon_i'\sum_j \epsilon_j'', \tag{3.36}$$

where $\epsilon_i'=\epsilon'(Z_i)$, and so on. The line shape is then simply found from $I(\Omega)$.

The difficulty of this calculation is that the contributions of the various defects to $\epsilon'\epsilon''$ do not simply add, although their contributions to ϵ' and ϵ'' separately are additive. For this reason, the analysis of Sec. 3.2 does not carry through, and further approximation is necessary. Here we give only a brief outline of the method, which is described in detail elsewhere.[57]

We can follow the previous section up to (3.17):

$$I(\Omega)=(v^{-1})^N\int dz_1 p(z_1)\cdots \times\int dz_N p(z_N)\,\delta[\Omega-\Omega(z_1,\cdots,z_N)]$$
$$=\frac{1}{2\pi}(v^{-1})^N\int_{-\infty}^{\infty}dx\exp(ix\Omega)\int dz_1 p(z_1)\cdots \times\int dz_N p(z_N)\exp[-ix\Omega(z_1,\cdots,z_N)]$$
$$=\frac{1}{2\pi}(v^{-1})^N\int_{-\infty}^{\infty}dx \times\exp(ix\Omega)\int dz_1\int dz_N\Phi(z_1,\cdots,z_N). \quad (3.37)$$

The difficulty is that Φ, given by

$$\Phi(z_1,\cdots,z_N)=p(z_1)\cdots p(z_N)\exp(-ix\sum_{i,j}\epsilon_i'\epsilon_j''), \quad (3.38)$$

does not factorise into N factors, each depending on only one of the z_i. This factorisation is crucial in Sec. 3.2, and is impossible here without further approximation.

There are three ways around this difficulty. Two of these avoid the statistical method altogether. Thus, one could assume some *qualitative* form for $I(\Omega)$ and then use the moments ($\langle\epsilon'\epsilon''\rangle$, for example) to fix the parameters which appear. This method has two difficulties: the moments can diverge (Sec. 3.3.1), and it is often hard to justify any particular qualitative form for $I(\Omega)$. The moment approach can sometimes be used when unresolved hyperfine structure causes broadening, but is rarely useful otherwise. The second method is to assume ϵ' and ϵ'' are uncorrelated and to find $I(\Omega)$ by a suitable convolution. This is often satisfactory for analysing data; one would, however, prefer a method which took the correlation of ϵ' and ϵ'' into account.

The third method is based on (3.37) and (3.38) and recognises that ϵ' and ϵ'' are not strictly independent. It is, however, still an approximate method. We first split $\Phi(z_1,\cdots,z_N)$ symmetrically into N factors f_i:

$$\Phi(z_1,\cdots,z_N)=\prod_{i=1}^{N}f_i,$$
$$f_i=p(z_i)\exp(-ix\epsilon_i'\epsilon_i'')\times\exp[-i(\tfrac{1}{2}x)(\epsilon_i'\sum_{j\neq i}\epsilon_j''+\epsilon_i''\sum_{j\neq i}\epsilon_j')]. \quad (3.39)$$

Each f_i depends on all the N coordinates $\{z_1,\cdots,z_N\}$ through the exponent:

$$ix\phi_i=ix(\tfrac{1}{2}\epsilon_i'\sum_{j\neq i}\epsilon_j''+\tfrac{1}{2}\epsilon_i''\sum_{j\neq i}\epsilon_j'). \quad (3.40)$$

The distribution of values of this exponent can be found from first-order theory; if we treat ϵ_i' and ϵ_i'' as known coefficients, then ϕ_i is simply a linear combination of the components of the local strain due to all defects but the ith. We now average each f_i over the distribution of values of the corresponding ϕ_i. The distribution of ϕ_i is given by

$$\tilde{I}(\phi_i)=\frac{1}{2\pi}\int_{-\infty}^{\infty}dy\exp(iy\phi_i)\exp[-\rho\tilde{J}_i(y)], \quad (3.41)$$

where

$$\tilde{J}_i(y)=\int du p(u)\{1-\exp[-iy\phi_i(u)]\} \quad (3.42)$$

and

$$\phi_i(u)=\tfrac{1}{2}[\epsilon_i'\epsilon''(u)+\epsilon_i''\epsilon'(u)]. \quad (3.43)$$

The averaged f_i is F_i, where

$$F_i\equiv\int d\phi_i\tilde{I}(\phi_i)f_i(\phi_i) \quad (3.44)$$

and replaces

$$f_i(\phi_i)=p(z_i)\exp[-ix(\epsilon_i'\epsilon_i''+\phi_i)]. \quad (3.45)$$

This is, loosely speaking, a random phase type of approximation. We replace the (exact) product of the f_i's by a product of averaged factors. The result is that F_i depends explicitly on z_i alone, the implicit dependence on the other $(N-1)$ coordinates being built into $\tilde{I}(\phi)$. Since N is large, we can ignore the fact that the average giving $\tilde{I}$ is over $(N-1)$ defects, rather than N. The product Φ is now effectively factorised, in that it is replaced by

$$\prod_{i=1}^{N}F_i(z_i).$$

Explicit calculation shows

$$F_i=p(z_i)\exp[-ix\epsilon'(z_i)\epsilon''(z_i)-\rho\tilde{J}(x,z_i)], \quad (3.46)$$

where $\tilde{J}(x)$ is given in (3.42) or, in more detail, as

$$\tilde{J}(x_i,z_i)=\int du p(u)\,(1-\exp\{-\tfrac{1}{2}ix[\epsilon_i'\epsilon''(u)+\epsilon_i''\epsilon'(u)]\}). \quad (3.47)$$

This method of averaging can also be used in more complicated cases with several second-order terms, e.g., $\epsilon'\epsilon''+\epsilon'''\epsilon''''$ replacing $\epsilon'\epsilon''$. The analogy with Sec. 3.2 can now be continued as the product can be factorised.

The result is

$$I(\Omega)=\frac{1}{2\pi}\int_{-\infty}^{\infty}dx\,\exp\,(ix\Omega)\,\exp\,[-\rho\Gamma(x)], \quad (3.48)$$

where

$$\Gamma(x)=\int dzp(z)\{1-\exp\,[-ix\epsilon'(z)\epsilon''(z)-\rho\tilde{J}(x,z)]\}. \quad (3.49)$$

These three equations summarise the second-order result. It is, of course, considerably more complicated than Sec. 3.2, and detailed justification and predictions are given in Ref. 57. One simple result can be derived however. By the use of the general expression for moments (3.25), we can verify that the result for the first moment $\langle\epsilon'\epsilon''\rangle$ is given as (3.34). A previous attempt to calculate second-order effects[20] dropped (3.40) altogether. This is equivalent to averaging the *exponent* in (3.39), rather than the whole product, and the result is inconsistent with (3.34). There seems to be no justification for this more drastic approximation.

3.4 Relation to Kubo–Tomita Theory

The three basic approaches in line-shape theory are the statistical method, the method of moments, and the Kubo–Tomita method.[25] The first two methods were compared briefly in Sec. 3.3.1; here we compare the statistical method with that of Kubo and Tomita, basing our argument on Ref. 26.

The Kubo–Tomita theory predicts a line shape

$$I_{\mathrm{KT}}(\omega)=\frac{1}{2\pi}\int_{-\infty}^{\infty}dt\,\exp\,(+i\omega t)\phi(t), \quad (3.50)$$

where $\phi(t)$ is the *relaxation function*

$$\phi(t)=\left\langle\exp\left(-i\int_0^t\tilde{\omega}(t)\,dt\right)\right\rangle. \quad (3.51)$$

The average is over an ensemble of the random process $\tilde{\omega}(t)$; the random process is supposed to be a *Gaussian* process. Thus, if $\omega_1,\cdots,\omega_N$ are the values of $\tilde{\omega}(t)$ at N arbitrary times, the probability that they lie in ranges $d\omega_i$ at ω_i $(i=1, N)$ is proportional to

$$\exp\,(-\tfrac{1}{2}\sum_{i=1}^{N}\sum_{j=1}^{N}a_{ij}\omega_i\omega_j)\,d\omega_1\cdots d\omega_N. \quad (3.52)$$

Further, the Gaussian process is *stationary* so that correlation functions like $\langle\tilde{\omega}(t+\tau)\tilde{\omega}(t)\rangle$ only depend on τ. The statistical method, on the other hand, is *static* rather than stationary; none of the variables are time dependent. Furthermore, the statistical method considers a *Poisson* process. All the ω_i are independent but are governed by the same distribution function. Equation (3.52) is replaced by the relation

$$\omega_i\equiv\epsilon(z_i),$$

and

$$P(z_1,\cdots,z_N)\,dz_1\cdots dz_N=\prod_{i=1}^{N}p(z_i)\,dz_i.$$

If the inhomogeneous and homogeneous mechanisms are independent, the resulting line shape is simply the convolution of $I_{\mathrm{KT}}(\omega)$ and the inhomogeneous line shape. This is valid when, for example, the transition probabilities giving homogeneous broadening do not vary appreciably with position in the inhomogeneous line. More formally we can write

$$I(\omega)=\frac{1}{2\pi}\int_{-\infty}^{\infty}dx\,\exp\,(ix\omega)\phi(x)\,\exp[-\rho J(x/\hbar\omega_1)]. \quad (3.53)$$

With this expression, there is no difficulty in going from the extreme of complete, homogeneous broadening to the opposite extreme of inhomogeneous broadening. This expression emphasises the value of working with the Fourier transform of the line shape, since it factorises into the product of a homogeneous part and an inhomogeneous part.

4. THE CONTINUUM APPROXIMATION

The assumptions of Sec. 3 are sufficient to derive general expressions for the line shape. To find the line shape explicitly in any real case we must, in addition, make assumptions about the specific forms of the perturbation field of the defects $\epsilon(z)$ and the statistical distribution of the defects $p(z)$. Here we review one very powerful set of assumptions and their application to various broadening mechanisms.

4.1 The Continuum Approximation

In this section we will assume that the lattice is an isotropic, homogeneous continuum. The perturbation fields we use will be the usual continuum elastic strain fields and the usual dielectric-continuum results for the electric fields and field gradients. The statistical distributions $p(z)$ will take no account of the lattice structure; the extension to include the discrete structure will be given in Sec. 5. Our only compromise with an exact treatment is to assume that the defects cannot approach within a radius R_1 of the centres whose transitions are observed and that the crystal has finite radius R_2. Wherever possible, however, we will assume R_1 zero and R_2 unlimitedly large.

A second approximation is that the defects are distributed completely randomly with respect to the centres observed. In principle there is no difficulty in dealing with other distributions apart from the problem of choice. In practice, however, the distributions of the defects may be strongly inhomogeneous (an example is the tendency of dislocations to form arrays and subgrain boundaries), and the centre whose transi-

tions are studied may be correlated with the defects. Bullough and Newman[58] review the interaction of point defects and dislocations and the cases where point defects are bound to the dislocations. The transitions of colour centres produced by irradiation may be broadened largely by the strain fields of point defects produced at the same time, and again some correlation of the centres and the defects may be expected. Similarly, when the random fields and field gradients of charged defects cause broadening, we may often expect the distributions of positively and negatively charged defects to be related for reasons of screening, in analogy with the case of ions in solution discussed by Debye and Hückel.

More generally, for point defects which interact with the centres, one should weight $p(z)$ by $\exp[-\phi(z)/kT]$, where T is the temperature and $\phi(z)$ the defect–centre interaction energy. This weighting is exact for two-body interactions $\phi(z)$ in the limit of low defect concentrations.[59,60] These two restrictions are closely related to the two assumptions of the statistical method contained in (3.9) and (3.10), i.e, the defects are uncorrelated and their contributions to the perturbation field are additive. The assumption of complete randomness is that $\phi(z)/k$ is much less than the lowest temperature at which the defects are mobile. The cases in which we might expect the assumption of randomness to be quite good are those in which the centres observed do not distort the lattice appreciably and have the same charge as the ions they replace. Transition-metal ions in MgO such as Fe^{2+}, Co^{2+}, and Mn^{2+} satisfy these requirements fairly well, as should F centres in alkali halides.

One further point common to all the cases to be discussed is the effect of the presence of the centre studied on the local properties of the lattice. Near the centre the elastic properties and the dielectric constant will be altered, and the question is whether these changes should be included in some way in calculating the line shape (i.e., the intensity as a function of energy). The answer is that these should *not* be included if the coupling coefficients used have been obtained by observing the changes in transition energy under externally applied electric fields or stresses. This is equivalent to the assumption that the local-field corrections needed because of the altered dielectric constant near the centre are the same for the uniform, externally applied field and for the nonuniform field due to a charged defect. The corresponding assumption in strain broadening is that the local change in force constant affects the response to an external applied stress and the stress field of a defect equally. These points can be checked using the statistical method, which shows that the perturbation field only varies appreciably over distances of the order of the mean defect separation. This is plausible intuitively, and it confirms that at low defect concentrations, the perturbation field is approximately uniform over the dimensions of one of the centres studies. Thus, in general, we will make no allowance for these local changes. As a result the widths of the deduced distributions of internal electric fields and internal strains will give "effective" internal fields and "effective" strains, the values which would give the correct local fields and atomic positions if there were no local changes, rather than the exact fields and atomic positions.

If, on the other hand, the coupling coefficients are theoretical estimates based on the exact configuration of the ligands or the exact applied field or field gradient then local corrections must be made. These are nearly always needed for the field-gradient case, as it is exceptionally difficult to measure the coupling coefficients directly. For the field and field-gradient cases, we may treat the centre whose transition is observed as a sphere of dielectric constant κ_1 in a lattice of static dielectric constant κ_2. The relation between the field V' and field gradient V'' with and without the local corrections is then[62,63]

$$V_L' = V_0'[(\kappa_1+2\kappa_2)/3\kappa_2] \tag{4.1}$$

and

$$V_L'' = V_0''[(2\kappa_1+3\kappa_2)/5\kappa_2]. \tag{4.2}$$

In these, the subscript L means the local corrections are included and the subscript 0 omits all local corrections. We will not give the corresponding results for strains. Not only are they more complicated, but their derivation uses more dubious assumptions about the boundary conditions between the host and the defect.

We now apply the theory to various broadening mechanisms. Detailed comparison with experiment is postponed until Sec. 6.

4.2 Strain Broadening by Dislocations[16,19,20]

In the simplest example we consider an elastically isotropic crystal in which the only strain sources are straight-edge or screw dislocations.[16] Each of the dislocations is described by five dislocations.[16] Each of the dislocations is described by five variables r, b, θ, ϕ, and α which correspond to the z_i used earlier. These variables are shown in Fig. 2 for screw dislocations. The variable r is the distance of the centre whose transition is observed to the nearest point of the dislocation line; b is the magnitude of the Burgers vector, and the dislocation axis **t** is specified by the angles θ and ϕ. For edge dislocations, α is the angle between **b** and **r**; for screw dislocations, α is shown in the figure. The angle α is only necessary because of the anisotropy of the dislocation strain field; the magnitude of a particular strain component referred to local axes at the centre studied is not given uniquely by r, b, θ, and ϕ.

It is an oversimplification to assume that the dislocations are pure edge or pure screw. A better assumption is that the Burgers vectors **b** of the dislocations

lie along a small number of directions determined by the crystal structure. For example, the Burgers vectors in MgO and Si (and analogous structures) are in the $\langle 110\rangle$ and equivalent directions and are of magnitude $\sqrt{2}a$ and $(2\sqrt{2}/3)a$, respectively, where a is the nearest-neighbour distance. The strain field of a dislocation whose axis makes an angle η with its Burgers vector is given by

$$e_{ij}=e_{ij}^{\text{screw}}\cos\eta+e_{ij}^{\text{edge}}\sin\eta, \tag{4.3}$$

where e_{ij}^{screw} and e_{ij}^{edge} are the strain fields of pure-edge and pure-screw dislocations with the same axis. The strain field is a more complicated function than before, as η is a function of θ, ϕ and $\mathbf{b}/|\mathbf{b}|$. Some caution must be taken to ensure α is defined consistently in e_{ij}^{screw} and e_{ij}^{edge}. We will write

$$\epsilon(z)=(b/\pi r)\psi(\theta,\phi,\alpha,\mathbf{b}/b) \tag{4.4}$$

for the strain field of a single straight dislocation in an elastically isotropic crystal. This form is sufficiently general to include the pure-screw and pure-edge cases, in addition to the more realistic example just described. The exact form of ψ will also depend on which particular combination of strain components is of interest as well as on the parameters describing the dislocation.

We assume that the dislocation distribution is statistically isotropic and homogeneous. By this we mean that the axes of the dislocations are distributed isotropically and that, for dislocations of given $\mathbf{b}$ and $\mathbf{t}$, the points of intersection of the dislocations with an arbitrary plane are distributed homogeneously on the plane. When we consider pure-edge dislocations we will also assume the Burgers vectors are isotropically distributed. For an isotropic distribution the probability that the dislocation axis lies within a particular solid angle is simply proportional to the solid angle, i.e., to $d\phi\,d\theta\sin\theta$. The probability of given values of r and α is proportional to $dr\,r\,d\alpha$ for a distribution which is homogeneous. Then integrals of the form $\int dz p(z)f(z)$, where f is an arbitrary function of z, should be interpreted as

$$\int_0^{\pi}d\theta\sin\theta\int_0^{2\pi}d\phi\int_0^{2\pi}d\alpha\int_{R_1}^{R_2}dr\,r f(\theta,\phi,\alpha,r) \tag{4.5a}$$

for pure-edge or pure-screw dislocations or

$$\sum_i F_i\int_0^{\pi}d\theta\sin\theta\int_0^{2\pi}d\phi\int_0^{2\pi}dx\times\int_{R_1}^{R_2}dr\,r f(\theta,\phi,\alpha,r,\mathbf{b}_i/|\mathbf{b}_i|) \tag{4.5b}$$

if the Burgers vectors are restricted to discrete values $\mathbf{b}_i$. In both these formulas we have omitted a constant of proportionality; this simply cancels out in the line shape. In the second expression we have assumed that the fractional probability that the Burgers vector lies along $\mathbf{b}_i$ is F_i, where

$$\sum_i F_i=1. \tag{4.6}$$

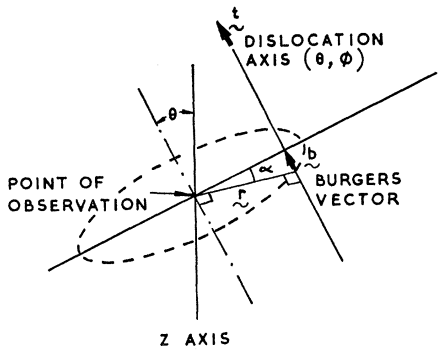

FIG. 2. The variables θ, ϕ, α, $\mathbf{r}$ and $\mathbf{b}$ for a screw dislocation.

In most of this section we will assume that the probability that there is a dislocation with vector $\mathbf{b}$ is exactly equal to the probability that there is a dislocation with vector $-\mathbf{b}$ but with the other parameters unaltered. This assumption is implicit in our assumption of isotropic axes and Burgers vectors for pure-edge or -screw dislocations, but it must be made explicitly when the Burgers vectors are only along discrete directions.

The lower limit R_1 on the radial integral can be used to take account of atomic structure of the lattice. We will find, however, that in calculating $I(\epsilon)$, it is a good approximation to put $R_1=0$. This would not be possible if we needed the moments of $I(\epsilon)$, since the strain field of the dislocation diverges as $1/r$ as r becomes small. The upper limit R_2 simply means that we consider a finite crystal; as R_2 becomes infinite, the usual logarithmic divergences met in dislocation theory appear. Since a finite crystal is considered, $I(\epsilon)$ will depend on the geometry of the surface and will be unreliable for the small values of ϵ (of order b/R_2, typically 10^{-6}) for which dislocations near the surface are particularly important. Recalling that linear elasticity [Eq. (3.9)] is only valid for strains ϵ less than about 10^{-2}, we see that the calculated distribution of strains $I(\epsilon)$ will only be reliable for

$$10^{-2}\geq\epsilon\geq10^{-6}. \tag{4.7}$$

The observed half-widths are typically 10^{-4}, so these inequalities do not cause much difficulty in practice.

In calculating ρ, $J(x)$, and $I(\epsilon)$, we will assume $R_1=0$. Thus, for a sphere of radius R we have

$$v=\int dz p(z)=4\pi^2R^2. \tag{4.8}$$

If the total length of dislocation per unit volume is L, including all possible Burgers vectors, the total length

of dislocation in the crystal is $\frac{4}{3}\pi R^3 L$. The number of dislocations N which pass through the sphere is $\frac{4}{3}\pi R^3 L/(\text{mean length of dislocation}) = \pi R^2 L$ for a homogeneous distribution, so

$$\rho = N \Big/ \int dz p(z) = \frac{L}{4\pi}. \tag{4.9}$$

This is, of course, independent of R.

$J(x)$ is given by Eqs. (3.22), (4.4), and (4.5). Thus, for the case in which the Burgers vectors are along specific directions only

$$J(x) = \sum_i F_i \int_0^{\pi} d\theta \sin\theta \int_0^{2\pi} d\phi \int_0^{2\pi} d\alpha \int_{R_1}^{R_2} dr\, d \times \{1 - \cos[x(b/\pi r)\psi(\theta, \phi, \alpha, \mathbf{b}_i/|\mathbf{b}_i|)]\}. \tag{4.10}$$

This is evaluated in Appendix I, where it is shown that for $R_1 = 0$

$$\rho J(x) = x^2 L b^2 (A - B \ln|x|), \tag{4.11}$$

in which

$$A = \{[0.9228 + \ln(\pi R_2/b)]I_2 + I_3\}(8\pi^3)^{-1},$$

$$B = I_2/8\pi^3,$$

$$I_2 = \sum_i F_i \int_0^{\pi} d\theta \sin\theta \int_0^{2\pi} d\phi \int_0^{2\pi} d\alpha\, |\psi|^2,$$

$$I_3 = \sum_i F_i \int_0^{\pi} d\theta \sin\theta \int_0^{2\pi} d\phi \int_0^{2\pi} d\alpha\, |\psi|^2 \ln|\psi|. \tag{4.12}$$

The line shape is given by our earlier result, (3.21), and (4.11), as

$$I(\epsilon) = \pi^{-1} \int_{-\infty}^{\infty} dx \cos\epsilon x \exp[-x^2 L b^2 (A - B \ln x)]. \tag{4.13}$$

If B were zero, this would describe a Gaussian shape, for which $\rho J(x)$ is proportional to x^2; the width of this Gaussian would be proportional to $L^{1/2}$, the square root of the dislocation density. The term $B \ln(x)$ reduces $I(\epsilon)$ at larger values of ϵ.

The *qualitative* form of $I(\epsilon)$ is determined by the integral over r in $J(x)$; the subsequent integrals over θ, ϕ, and α affect the magnitudes of the parameters A and B, but do not affect the functional form of $I(\epsilon)$. Thus, if the observed shape of a resonance line is attributed to broadening by dislocations alone and it has a shape qualitatively different from (4.13), then either the dislocation distribution is inhomogeneous or the centres observed are correlated in position with the dislocations. If the correlation is important, both the line shape and its width should differ from the values predicted without it.

The assumption of isotropy for the dislocation distribution can be checked less directly. If $I(\epsilon)$ can be measured for several different combinations of strain components (ϵ, ϵ', ϵ'', $\cdots$, etc.), then the relative widths of the corresponding distributions are sensitive to the extent to which the dislocation distribution is anisotropic.

We may also estimate the shift of the resonance line when Burgers vectors $\mathbf{b}$ and $-\mathbf{b}$ are not equally probable. In this case we must find the imaginary part of $J(x)$ which is, using (4.3a),

$$\mathrm{Im}\, J(x) = \sum_i F_i \int_0^{\pi} d\theta \sin\theta \int_0^{2\pi} d\phi \int_0^{2\pi} d\alpha \int_{R_1}^{R_2} dr\, r \times \sin[x(b/\pi r)\psi]. \tag{4.14}$$

This is calculated in Appendix I, where it is shown that

$$\rho\, \mathrm{Im}\,(J) = x\left[\frac{LRb}{4\pi} \sum_i F_i \int_0^{\pi} d\theta \times \sin\theta \int_0^{2\pi} d\phi \int_0^{2\pi} d\alpha p_i(\theta, \phi, \alpha)\psi(\theta, \phi, \alpha, i)\right] = x\Delta, \tag{4.15}$$

in which $p_i(\theta, \phi, \alpha)$ describes the (possibly anisotropic) dislocation distribution; in the isotropic case $p = 1$. We see from (3.20) that the resonance line is shifted *rigidly* by an amount $-\Delta$ proportional to L, b, and the crystal dimension R. The shift is only finite if p_i depends on all of θ, ϕ, and α. Thus, the distribution of the dislocation axes (given by θ, ϕ) must be anisotropic, and the defect distribution must also be inhomogeneous, so that p_i depends on α.

Crystals containing anisotropic, inhomogeneous dislocation distributions usually show macroscopic distortion. Faces which would be parallel in a perfect crystal have slight angles between them. The angle for any given pair of faces is proportional to $LRbf$, where R is the separation of the faces and the numbers of dislocations with Burgers vectors $+\mathbf{b}$, $-\mathbf{b}$ are in the ratio $(1+f):(1-f)$. Thus, the shift of the resonance line, Δ, is proportional to the change in the angle between two of the external faces of the crystal. The constant of proportionality depends on the choice of faces and the $p_i(\theta, \phi, \alpha)$. This proportionality is similar to results for other broadening mechanisms where the shift proves to be proportional to some macroscopically measureable quantity.

Strain broadening by dislocation dipoles: A dislocation dipole is a pair of dislocations with parallel axes and opposite Burgers vectors. Its strain field has the following form at large distances r from the dipole:

$$\epsilon(z) = (bl/r^2)\psi(\theta, \phi, \alpha, \beta, \mathbf{b}_i/|\mathbf{b}_i|),$$

where all the variables except l and β are the same as in the previous discussion; l is the separation of the dislocations which constitute the dipole, and β specifies

the orientation of the dipole. We show that unless essentially every dislocation in a crystal is paired to form a dipole, their contribution to the broadening is negligible (contrary to the result of Ref. 20). We will also show that the results give an alternative procedure to that used in the discussion of dislocations (where we assumed a finite crystal) for removing the apparent divergence at large R_2.

In Appendix II we show that dipoles give a Lorentz line of width

$$(L/32\pi)\mid bl\mid\sum_i\int_0^{2\pi}d\phi\int_0^{2\pi}d\alpha\int_0^{2\pi}d\beta\int_0^{\pi}d\theta\cos\theta\mid\psi\mid$$

if we were to assume the long-range form of $\epsilon(z)$ valid for all r. The width is thus of order Lbl, as opposed to order $10bL^{1/2}$ for isolated dislocations. Dipoles are only important if $lL^{1/2}$ is large, and this is rarely the case. If a fraction $(1-f)$ of the dislocations in a crystal form components of dipoles and a fraction f are present as single dislocations, their respective contributions to the width are $\frac{1}{2}(1-f)Lbl$ and $10fLb$. The dipolar contribution is largest when

$$lL^{1/2}/20>f^{1/2}/(1-f).$$

With $l=100$ Å and $L=10^{12}$ cm/cc, the dipolar contribution dominates only if less than one-quarter of 1% of the dislocations are present as isolated dislocations. Dipoles can certainly be neglected at reasonable densities in real crystals.

We may, however, take advantage of the r^2 falloff of the dipole strain field at large r to avoid the divergence at large R_2 for isolated dislocations. The method we describe has no major advantages but provides an alternative which may be useful in some cases. For our dislocation distribution we assume that for each dislocation with a given axis and Burgers vector **b** there is another dislocation with a parallel axis and Burgers vector $-\mathbf{b}$. We assume that on the average, the separation of these dislocations is R_2, of the order of normal crystal dimensions. For $r\ll R_2$ we may neglect the correlation between the dislocations and repeat the discussion as if for isolated dislocations. For $r\gg R_2$, however, the r^{-2} falloff means that the divergence at large r is eliminated without the need to introduce the singularity of a crystal boundary. The separation R_2 is now interpreted as a correlation length rather than a crystal size.

4.3 Broadening Due to Point Defects by Random Strains and Field Gradients[9,17,18]

A point defect can perturb other centres by a number of different mechanisms: by the electric field or field gradient of the defect or by mechanical distortion which gives a strain field. For several cases the perturbation fields $\epsilon(z)$ are qualitatively identical. The continuum form of the distribution function $p(z)$ is, of course, independent of the mechanism of interaction, so we may treat all these mechanisms together.

The variables z for point defects are the Cartesian coordinates (x_i, y_i, z_i) or polar coordinates (r_i, θ_i, ϕ_i) of the defect with respect to the centre studied. We will label the different species of point defects in any one crystal by k.

Since the defects are randomly distributed, we have

$$p(z)\,dz\sim r^2\,dr\,d\phi\sin\theta\,d\theta, \tag{4.16}$$

and $\rho\equiv N/\int dzp(z)$ is simply the number of defects per unit volume. The perturbation fields we consider in this section all have the form

$$u_{\alpha\beta}\equiv A_k(1/r^3)[\delta_{\alpha\beta}-3(x_\alpha x_\beta/r^2)]=A_k[\psi_{\alpha\beta}(\theta,\phi)/r^3], \tag{4.17}$$

where A_k is the strength of the defect. This *excludes*, for example, broadening due to random electric field of charged defects, which have a different form for $\epsilon(z)$; these will be treated in Sec. 4.4.

It is convenient to distinguish between *strain broadening* and *electric-field-gradient broadening*. The distinction is an artificial one in the sense that even uncharged defects perturb other centres by disturbing the distribution of the electronic and nuclear changes near the centre, and the disturbance can be represented (to lowest order) by a field gradient. The division into two types of mechanism—the effect of local strain and the direct effect of the defect charge—is useful for two reasons. First, the response of a centre to strains is usually measured directly by observing the resonance of a centre under external stress; the response to a field gradient is usually calculated theoretically and so needs some sort of local-field correction. In NMR, additional corrections are needed for antishielding and covalency effects.[9] Second, sources of strain (which may or may not be charged) produce changes in the x-ray lattice parameter and macroscopic size of the crystal. Charged defects which have the same ionic radius as the ions they replace will only change the lattice parameter if the crystal has a net charge; usually, crystals are electrically neutral because of charge compensation, so no alteration of lattice parameter would be expected.

The two extreme cases are sometimes described as the "size" and "charge" effects. They are the following:

(i) *Strain broadening.* A_k is the strength of the defect, usually of order a^3, where a is the nearest-neighbour distance of the host lattice. In this case,

$$u_{\alpha\beta}\equiv e_{\alpha\beta},$$

where e is the strain tensor, and we calculate the distribution of the dimensionless scalar

$$\epsilon=\sum a_{\alpha\beta}u_{\alpha\beta}\equiv\sum a_{\alpha\beta}e_{\alpha\beta}. \tag{4.18}$$

The strength of the defect A_k is related to the volume

dilation per defect B_k by

$$B_k=\frac{4\pi A_k\{1+2[(1-2\nu)/(1+\nu)]\}}{\Omega}$$
$$=12\pi[(1-\nu)/(1+\nu)](A_k/\Omega), \quad (4.19)$$

where we have assumed linear isotropic elasticity theory and that the crystal has a large but finite radius; Ω is the atomic volume and ν is Poisson's ratio. These expressions are most nearly exact in cases where the impurity has the same charge as the ion or atom it replaces, for example, K^+ in NaCl or Si in Ge.

The other extreme is

(ii) *Field-gradient broadening* from the direct effect of the defect treated as a point charge. This is the important mechanism when the net charge of the defect differs from that of the ion it replaces (if any), but which causes no appreciable strain; that is, the atomic volumes of the displaced ions and the defect are closely similar. Fe^{3+} in MgO is quite a good example. If we expand the potential due to a defect about a centre at $\bar{\mathbf{x}}=0$, then

$$V=V(0)+\sum_\alpha \bar{\mathbf{x}}_\alpha(\partial V/\partial\bar{\mathbf{x}})_\alpha+\sum_{\alpha,\beta}(e/a^3)\tfrac{1}{2}u_{\alpha\beta}\bar{\mathbf{x}}_\alpha\bar{\mathbf{x}}_\beta+\cdots. \quad (4.20)$$

The first term $V(0)$ does not affect the transition energy. The second term, which gives the local electric field, only affects the transition energy to first order in special circumstances; these will be treated in more detail in the next section. The third term, giving the electric field gradient, is the one of interest here.

If the defect charge differs from that of the ion it replaces by $Z_k\,|\,e\,|$, then the field gradient has the form

$$V_{\alpha\beta}\equiv\frac{|\,e\,|}{a^3}\frac{Z_k}{\kappa_{\rm eff}}\frac{\psi(\theta,\phi)}{(r/a)^3}.$$

It is simpler to calculate the distribution of a dimensionless quantity, so we find the distribution of the field gradient in units of $|\,e\,|/a^3$. The strength of the defect is then $A_k\equiv Z_k a^3/\kappa_{\rm eff}$. The effective dielectric constant is the static constant κ_0; if local corrections are needed, then $\kappa_{\rm eff}=(3\kappa_0+2)/5$, using (4.2) with $\kappa_2=\kappa_0$ and $\kappa_1=1$.

In general, neither of these extremes is exact and considerable care is needed in defining the strength A_k. This difficulty has been recognised for a long time in attempts to calculate defect strengths, interaction energies, and formation energies, and systematic treatments of the electrical and mechanical effects are only now becoming available.[64] One result is that it may be hard to predict *shifts* of resonance lines accurately; there are terms which appear in the strain case because the crystal is finite, but not in the field-gradient case, and which may give difficulties in practice [see (4.23)].

(iii) *Magnetic dipole broadening.* As this has been treated in great detail by Grant and Strandberg[14] we simply draw attention to the close relation of their work to the mechanisms treated in this section.

(iv) *Field broadening from an electric dipole.* This will only be observed for centres without inversion symmetry. For other centres the coupling coefficient $\hbar\omega_1$ vanishes for reasons of parity. We define A_k as $Z_k\,|\,e\,|\,\Lambda_k a^2/\kappa_{\rm eff}$ and calculate the distribution of some combination of field components $E_\alpha(\,|\,e\,|/a^2)^{-1}$. The dipole moment of the defect is $Z_k\Lambda_k\,|\,e\,|$, and $u_{\alpha\beta}$ is the β component of $\mathbf{E}(\,|\,e\,|/a^2)^{-1}$ due to the α component of the electrical dipole moment; $\kappa_{\rm eff}$ here is κ_0 or $\kappa_0/\frac{1}{3}(\kappa_0+2)$ depending on whether the local-field corrections are needed or not.

The line shape is calculated in Appendix II using (4.16) and (4.17). $I(\epsilon)$ proves to be Lorentzian with full width at half-intensity

$$\tfrac{1}{3}\pi\left(\int_0^\pi d\theta\sin\theta\int_0^{2\pi}d\phi\,|\,\psi(\theta,\phi)\,|\,\right)\sum_k\rho_k\,|\,A_k\,| \quad (4.21)$$

shifted from its unperturbed position by

$$-\frac{1}{3}\left(\int_0^\pi d\theta\sin\theta\int_0^{2\pi}d\phi\psi\ln|\,\psi\,|\,\right)\sum_k\rho_k A_k. \quad (4.22)$$

We give here the results generalised to cases where there are several species of point defect present; ψ is $\sum_{\alpha,\beta}a_{\alpha\beta}\psi_{\alpha\beta}$ by (4.18). The width and the shift are both *linear* in the defect concentration.

Equation (4.22) is incomplete for strain broadening in a finite crystal. The reason is that in a finite crystal there must be no surface tractions on the free surface. The main consequence is, as Eshelby showed,[65] a uniform dilatation[66] such that (in Cartesian coordinates)

$$e_{ii}=(8\pi/3)[(1-2\nu)/(1+\nu)]\sum_k A_k\rho_k,$$

where ν is Poisson's ratio. The amended version of (4.22) is

$$\left(\frac{8\pi}{3}\frac{1-2\nu}{1+\nu}\sum_\alpha a_{\alpha\alpha}-\frac{1}{3}\int_0^\pi d\theta\sin\theta\int_0^{2\pi}d\phi\psi\ln|\,\psi\,|\,\right)\times\sum_k\rho_k A_k. \quad (4.23)$$

The "Eshelby" term is more likely to be important in optical transitions than in spin resonance. In spin resonance the transition is one between states which mainly differ in spin alone, so the transition is less sensitive to hydrostatic pressure; $\sum_\alpha a_{\alpha\alpha}$ is small. Optical transitions are between different electronic configurations and may be very sensitive to hydrostatic pressure (see Sec. 6.3, where the Eshelby term gives over 80% of the total shift).

As in the case of dislocations, the shift is proportional to another measureable quantity; for strain broadening this is the fractional change in x-ray lattice parameter, $\Delta a/a$. This and the fractional change in macroscopic length, $\Delta L/L$, are often measured in studies of radiation damage.[67,68] They are given by

$$\delta L/L=\tfrac{1}{3}[\rho_i(B_i-1)+\rho_v(B_v+1)]\Omega,$$
$$\delta a/a=\tfrac{1}{3}(\rho_i B_i+\rho_v B_v)\Omega, \quad (4.24)$$

when specialised to the case where vacancies (v) and interstitials (i) alone are present. It is clear that the linewidth (4.21) gives information additional to $\delta L/L$ and $\delta a/a$ as it only involves the *magnitudes* of the strengths of the defects, $|A_k|$. This should be particularly valuable in cases (as in Si and Ge) where A_i and A_v have different signs.

4.4 Broadening by Random Electric Fields[15]

Since the electric field at a defect is a vector, it has odd parity. The transition energy of a centre will only change linearly with the field if the centre itself lacks inversion symmetry so that its eigenstates have no definite parity, or if there is a very close[69] state with opposite parity to one of those between which the transition occurs. For this reason far fewer centres are sensitive to random electric fields than to strains or field gradients.

As in the previous section (Sec. 4.3) the distribution of the point defects which cause the broadening is

$$p(z)\,dz = r^2\,dr\sin\theta\,d\theta\,d\phi; \tag{4.25}$$

ρ is again the number of defects per unit volume. The perturbation is some linear combination of the components of the electric field from one of the defects so that we can always write ϵ in the form

$$b_xE_{xi}+b_yE_{yi}+b_zE_{zi}=\mathbf{b}\cdot\mathbf{E}_i,$$

where $\mathbf{b}$ is a unit vector. If we choose $\mathbf{b}$ to be the polar axis $\theta=0$, then

$$\epsilon_i\sim|E_i|\cos\theta_i=(-Z_i|e|/\kappa_0)(\cos\theta/r_i^2).$$

As it is convenient to make ϵ dimensionless, we express the electric field in units of $|e|/\kappa_0a^2$, so

$$\epsilon(z_i)=-Z_ia^2\cos\theta_i/r_i^2. \tag{4.26}$$

We have included *no* local-field corrections in this expression. The line shape is evaluated in Appendix IV. The main features are that the shape is that sometimes known as the *Holtsmark* distribution,[70]

$$I(\epsilon)=\frac{1}{2\pi}\int_{-\infty}^{\infty}dx\exp(ix\epsilon)\exp[-A(x)^{3/2}], \tag{4.27}$$

which is intermediate between a Lorentzian and a Gaussian, and that there is *no* shift of the line. The absence of a shift is a direct consequence of our simple-continuum approximation (4.25) in which inversion symmetry is implicit. The shift comes from a term in $\rho J(x)$ which is

$$i\rho\int_0^{2\pi}d\phi\int_{-1}^{+1}d(\cos\theta)\int_{R_1}^{R_2}drr^2\sin\left(\frac{-z\cos\theta}{r^2}x\right);$$

the integral over θ vanishes because the integrand is an odd function of $\cos\theta$. In the discrete-lattice case (Sec. 5) the corresponding term does not vanish. The linewidth of the distribution of electric fields is[71]

$$7.5(|e|/\kappa_0)(\sum_k\rho_k|Z_k|^{3/2})^{2/3}, \tag{4.28}$$

where we have generalised the result to apply when there are several defects of different charge present.

Despite the relatively complex form, several features found in the previous cases recur. First, the width depends only on the *magnitudes* of the charges and not on their signs. Second, if we keep the distribution unaltered and simply scale the strengths of the defects, the linewidth scales in exactly the same way.

It is sometimes convenient to measure the peak-to-peak differential width Δ' of a resonance line instead of its full width at half-intensity, Δ. For the shape given by (4.27), Δ/Δ' is 1.309, compared with 1.732 for a Lorentzian and 0.9901 for a Gaussian.

4.5 Asymptotic Results at Large Perturbations

The line shape $I(\epsilon)$ can be derived very directly when the perturbation field ϵ is large. In practise, the results are only of use in the case of strain broadening by dislocations, for in other cases the breakdown of the continuum approximation leads to the appearance of structure and satellite lines.

It is assumed that the contribution of one defect alone dominates at large perturbations. Configurations in which several defects are close to the centre studied are ignored; this has some justification from the assumption of low defect concentrations.

The probability that the *nearest* defect to the centre studied lies between R and $R+dR$ of the centre is $W(R)\,dR$, normalised so that

$$\int_0^{\infty}dRW(R)=1.$$

If $p(z)\,dz$ is proportional to $R^n\,dR$, then

$$W(R)\sim R^n\left(1-\int_0^R drW(r)\right),$$

where the second factor is the probability that there is no defect closer than R. If the distribution is not completely random (for example, of the defect and centre interact with an interaction energy depending on R), then we should include an extra function $\phi(R)$ in $p(z)$.

At very small R the integral

$$\int_0^R drW(r)$$

is negligible, and $W(R)\sim R^n$. In the same range the perturbation $\epsilon(z)$ varies as R^{-m}. The long-range continuum approximation for ϵ will be used here, although it is straightforward to treat a more general interaction. We can write $\epsilon\sim R^{-m}$ as $R\sim\epsilon^{-1/m}$, so $R^n\,dR$ can be written as $(\epsilon^{-1/m})^n\epsilon^{-1-1/m}\,d\epsilon$. Since $I(\epsilon)\,d\epsilon$ is pro-

TABLE I. Data used in estimating the ranges of importance of the various mechanisms. The sources are given in Ref. 72.

Property	Si	MgO
Static dielectric constant K_0	12.0	9.8
Nearest-neighbor distance a (Å)	2.35	2.104
(Volume per atom/a^3) $= V/a^3$	1.54	2.00
Burgers vector (Å)	3.84	2.975
$\Delta V/V$ for neutral or anion vacancy	+0.6(72a)	−0.4(72b)
Poisson's ratio [Voigt average (72c)]	0.218	0.172

portional to this,

$$I(\epsilon)\, d\epsilon \sim (1/\epsilon^{1+(n+1)/m})\, d\epsilon.$$

This is the asymptotic form of $I(\epsilon)$, valid when the perturbation is so large that one close defect dominates, yet where the discrete crystal structure is not important. For the specific cases of interest the results are as follows:

(a) Strain broadening by dislocation ($n=m=1$);

$$I(\epsilon)\sim\epsilon^{-3}.$$

(b) Strain broadening by point defects and equivalent cases ($n=2$, $m=3$);

$$I(\epsilon)\sim\epsilon^{-2},$$

as expected for a Lorentzian line (Sec. 4.3).

(c) Electric-field broadening ($n=m=2$);

$$I(\epsilon)\sim\epsilon^{-5/2}.$$

It is hard to check these experimentally because the wings of the resonance line are usually obscured by noise and by other transitions. The 5234-Å line due to N centres in LiF [54] appears to be strain broadened by dislocations, and its wings (i.e., beyond the points of half-intensity) fall off roughly as ϵ^{-M}, where $4.5\geq M\geq 2.5$. If this does illustrate the asymptotic form, then the result suggests that the strain field diverges less rapidly than $1/R$ near the dislocation, thus raising M slightly. In practice, the technical difficulty of analysing the data makes it hard to be sure that the region of validity of the asymptotic form has been reached.

4.6 Ranges of Importance

Here we attempt to outline the circumstances in which one would expect to detect one mechanism rather than another. In general, it should be possible to detect inhomogeneous broadening when the perturbation distributions have the following half-widths:

(i) strains	$\gtrsim 10^{-4}$;
(ii) electric fields	$\gtrsim 10^5$ V/cm;
(ii) electric field gradients	$\gtrsim 2.10^{13}$ V cm$^{-1}\cdot$cm^{-1} $\sim 5.10^{-4}(e/a^2)$.

The inhomogeneous contribution may, of course, be hidden by relaxation broadening or other effects. We now calculate defect densities which give distributions with these widths.

The circumstances which determine the relative importance of the different mechanisms depend on the defect species and the host lattice. To some extent they also depend on the centre studied, in that electric fields do not broaden lines from centres with inversion symmetry to first order. Rather than present a multitude of calculations for different defect species, centres, and hosts, we present a set of "typical" results for silicon and magnesium oxide. Thus, we calculate the concentration of a particular defect which gives a distribution of the width quoted above. The data used are given in Table I[72]; no local field corrections are included, so these results may underestimate the electric-field-gradient contribution:

(i) Strain broadening:

	Dislocation density	*Point defects*
Si	7×10^5 cm/cc	40 ppm (neutral vacancy)
MgO	10^6 cm/cc	70 ppm (anion vacancy).

(ii) Electric-field broadening by charges Ze:

Si	$Z=1$	30 ppm
MgO	$Z=1$	11 ppm
	$Z=2$	4 ppm.

Very few centres in MgO lack inversion symmetry. The R-like colour centres of Ref. 33 lack it and may be sensitive to electric fields.

Very small defect concentrations are needed to give large random fields. It may be possible to use these random fields to test the symmetry of centres under inversion. This is an extension of more direct Stark effect experiments which suffer from the difficulties of applying really large external electric fields:

(iii) Field-gradient broadening by charges Ze:

Si	$Z=1$	130 ppm
MgO	$Z=1$	80 ppm
	$Z=2$	40 ppm.

5. THE DISCRETE LATTICE

It is clear from our discussion of the isotropic continuum case that while the results were suggestive, they would be invalid in real crystals because of the atomic structure of the lattices. Corrections are necessary for both the perturbation fields of the individual

defects $\epsilon(z)$ and for the distribution of the defects with respect to the centres observed, given by $p(z)$. The effects of these changes are discussed here.

5.1 Qualitative Features

The continuum formulae for $\epsilon(z)$ fail in two respects. First, they should be adequate at large distances from the defect, but short-range corrections will be necessary. The exact form of the corrections will depend on the details of the defect and the lattice; such corrections are found (in principle, at least) in atomistic calculations for defects.[73] In cases where these calculations have not been made, the $\epsilon(z)$ may be treated as empirical parameters. The second failure of the simple continuum $\epsilon(z)$ is that it neglects the *microscopic* anisotropy of all crystal lattices (even those which are isotropic in macroscopic elasticity). In principle, of course, anisotropy can be included in a continuum model; in practice the problem is intractable. Thus, some lines which are not broadened in a continuum treatment may be broadened in this more exact approach. An example would be a line which shifted linearly with the dilatation

$$\hbar\omega=\hbar\omega_0+\hbar\omega_1(e_{xx}+e_{yy}+e_{zz}).$$

In an isotropic, homogeneous continuum containing only point defects the line would be sharp, as $e_{xx}+e_{yy}+e_{zz}$ is constant in space. In a real crystal, however, the dilatation is not constant and the line will be broadened. We will assume in this section that $\epsilon(z)$ is a known function of z, and we will continue to assume that the contributions of the various defects to ϵ simply add linearly. It is, in fact, no longer obvious that, for example, linear elasticity is still valid very near to the defects we are considering, and we will return to the question of nonlinear effects later.

The statistical distribution function $p(z)$ also differs from its continuum value. The microscopic *anisotropy* of the lattice is again important. In our discussion of electric-field effects we found that the resonance line was not shifted and that it was symmetric simply because of the implicit inversion symmetry of the lattice. Real lattices often lack this symmetry, so that we may expect to find asymmetric or shifted lines in practice. The *inhomogeneity* of the lattice has a more profound effect. Essentially, the function $p(z)$ has sharp peaks which lead to structure in the resonance lines. For example, if the defects are substitutional point defects, $p(z)$ is only finite when $z\equiv(\mathbf{r},\eta)$ corresponds to a lattice site. This often leads to structure in the form of satellite lines, and these have been observed in NMR,[74–76] in EPR,[77–79] in optical absorption by colour centres[80,81] and transition-metal ions,[82] and in Mössbauer transitions. In the case of strain broadening by dislocations, we do not expect to see such satellites. The atomic structure of the lattice does, of course, limit the values of $\mathbf{r}$ for which $p(z)\equiv p(\mathbf{r},\eta)$ is finite to certain discrete positions. However, for a given $\mathbf{r}$ there is an essentially continuous distribution of the other variable η which gives the axis of the dislocation and the direction and magnitude of its Burgers vector. The distribution in η smears out any structure of the line. In our discussion in Secs. 5.2 and 5.3 we will concentrate entirely on point defects.

5.2 The Structure of the Resonance Line[14]

In this section we show the origin of satellite lines in more detail. We divide the crystal around the centres whose transitions are observed into two regions. For defects in the inner region (region I) the lattice is treated as discrete, and in the outer one (region II) we use the continuum approximations outlined in Sec. 4. As a rough criterion in choosing the boundary between the regions we may require that if we treated the whole crystal as discrete and if there were *no* defects in the inner region, then the resulting line shape should show no significant resolvable structure.

In the inner (discrete) region the continuum forms of $p(z)$ and $\epsilon(z)$ are not valid. We will define two corresponding functions f_z and ϵ_z; f_z is the fractional probability that there is a defect at the discrete site $\mathbf{r}$ in the discrete state η. The correspondence between f and p is that $f_z\equiv\rho p(z)\,dz$. Similarly we will replace $\epsilon(z)$ by ϵ_z and assume that f_z and ϵ_z are known (here unspecified) functions of z. Care must be taken in defining ϵ_z; for example, the strains in the continuum case must be properly defined in terms of relative displacements in the discrete case. The line shape is again given by

$$I(\epsilon)=\frac{1}{2\pi}\int_{-\infty}^{\infty}dx\,\exp\,(ix\epsilon)\,\exp\,[-\rho J(x)], \quad (5.1)$$

in which $\rho J(x)$ is now given by

$$\rho J(x)=\sum_{\mathrm{I}} f_z[1-\exp\,(-ix\epsilon_z)]$$

$$+\rho\int_{\mathrm{II}} dzp(z)\{1-\exp\,[-ix\epsilon(z)]\}$$

$$\rho J(x)=-\sum_{\mathrm{I}} f_z\exp(-ix\epsilon_z)$$

$$+\left(\sum_{\mathrm{I}} f_z+\rho\int_{\mathrm{II}} dzp(z)\{1-\exp\,[-ix\epsilon(z)]\}\right)$$

$$=-\sum_{\mathrm{I}} f_z\exp\,(-ix\epsilon_z)+\rho J_c(x). \quad (5.2)$$

We have transferred $\sum_{\mathrm{I}} f_z$, the probability that there is a defect in region I, to the continuum-contribution to $\rho J_c(x)$ simply because we will find later that there is a term in the contribution from region II with which it tends to cancel. It is a constant and, in any case, makes essentially no difference to the line shape or

width. Substituting (5.2) in (5.1)

$$I(\epsilon)=\frac{1}{2\pi}\int_{-\infty}^{\infty}dx\exp(ix\epsilon)\exp\Big[+\sum_{\mathrm{I}}f_z\exp(-ix\epsilon_z)\Big]\times\exp[-\rho J_c(x)]$$

$$=\frac{1}{2\pi}\int_{-\infty}^{\infty}dx\exp(ix\epsilon)\exp[-\rho J_c(x)]\times\Big[1+\sum_{\mathrm{I}}f_z\exp(-ix\epsilon_z)+\cdots\Big]$$

$$=\frac{1}{2\pi}\int_{-\infty}^{\infty}dx\exp(ix\epsilon)\exp[-\rho J_c(x)]$$

$$+\sum_{\mathrm{I}}f_z(2\pi)^{-1}\int_{-\infty}^{\infty}dx\exp[ix(\epsilon-\epsilon_z)]\exp[-\rho J_c(x)]$$

$$+\tfrac{1}{2}\sum_{\mathrm{I}}f_{z_1}f_{z_2}(2\pi)^{-1}\int_{-\infty}^{\infty}dx\exp[ix(\epsilon-\epsilon_{z_1}-\epsilon_{z_2})]\times\exp[-\rho J_c(x)]+\text{higher terms.}\quad(5.3)$$

In expanding the exponential, low concentrations are assumed so that the f_z are small. The final expression (5.3) shows that $I(\epsilon)$ consists of a main line (given by the first term) on which is superposed satellite lines with the same shape and of relative intensity f_z centred on ϵ_z, and so on. The assumption of low concentrations actually takes a slightly different form here than in the discussion of Sec. 3. Here we want the f_z small so that only a few terms in (5.3) need be considered. In Sec. 3 we wanted the distribution of the defects to factorise into a product of factors such as $p(z)$, and configurations in which two defects were at the same lattice site caused difficulty. In the expansion in (5.3), it is trivial to exclude such configurations by omitting terms which contain squares or higher powers of f_z for any particular z.

The expansion also suggests that a Monte Carlo treatment might give useful results. This would calculate ϵ for a large number of randomly selected configurations of defects within a relatively large region I. Such a calculation has been made in Ref. 79 for the line shape of Cr^{3+} in $ZnWO_4$ and was able to predict the appearance of satellite lines.

5.3 Relation to the Continuum Approximation

The shape of the main line is given by

$$I_M(\epsilon)=\frac{1}{2\pi}\int_{-\infty}^{\infty}dx\exp(ix\epsilon)\exp[-\rho J_c(x)].\quad(5.4)$$

Apart from a rigid shift and corrections for nonlinear terms, discussed later, the shape of the satellites is given by the same function. This line shape is, in general, different from the line shape $I_0(\epsilon)$ calculated using the continuum approximation for the whole crystal. The exclusion of region I in calculating $\rho J_c(x)$ is reflected in the line shape $I_M(\epsilon)$. What we find, however, is that $I_0(\epsilon)$ and $I_M(\epsilon)$ will often be sufficiently similar so that for practical purposes we may ignore the difference between them. Qualitatively the reason is this. The usual choice of the region to be treated discretely is the region within a sphere of radius R of the centre observed. If R is reasonably small, then a defect at most of the sites within the sphere would produce a large perturbation, appreciably larger than the perturbation corresponding to the half-width of the line. Thus, on the whole, the elimination of the region I only affects the far wings of the resonance line, and changes here are generally unobservable. This argument is, of course, an oversimplification. Defects at some positions within R sometimes produce small perturbations, usually for symmetry reasons. By eliminating region I in calculating $I_M(\epsilon)$ we expect to find differences between $I_M(\epsilon)$ and $I_0(\epsilon)$ of the order of the fraction of the defect configurations which have defects at sites within R giving small perturbations. This fraction is generally small and independent of concentration for random defects.

Exactly the same conclusions hold quantitatively. When $J_c(x)$ is calculated explicitly (as in the Appendices), we find ρJ_c differs from its value when $R=0$ by two types of term. The first is $(\sum_z f_z-\frac{4}{3}\pi R^3\rho)$, which is identically zero for a completely random defect distribution and which, in any case, only introduces a constant factor into $I_M(\epsilon)$. The second type of term vanishes when $R=0$ and may be expanded as a function of $1/x\epsilon(R)$. Here $\epsilon(R)$ is the perturbation in the continuum approximation for a defect at the boundary between regions I and II. In general $\epsilon(0)$ is infinite. As the line shape is found from the Fourier transform (5.1), the half-width of the line $\epsilon_{1/2}$ is of order $1/x$, so the expansion parameter is $\epsilon_{1/2}/\epsilon(R)$. Again we see that those defect positions where $\epsilon(R)$ is small cause problems, but that in general $\epsilon_{1/2}/\epsilon(R)$ is small if R is small. Estimates of upper limits for R for this expansion to be acceptable are generally in the region of 10–15 Å. As a working approximation we find, therefore, that the shape of the main line $I_M(\epsilon)$ is usually given to sufficient accuracy by the continuum approximation with $R=0$.

Nonlinear effects may cause deviations from this rule for the satellite lines which, from (5.3), should have the same shape as the main line. As the perturbation from a nearby defect is usually large the defect may cause changes in the local elastic constants or dielectric constants. These will primarily affect the coupling coefficients, $\hbar\omega_1 a_{ij}$ or $\hbar\omega_1\alpha_j$ of (3.1) and (3.2). The main result is likely to be a change of scale of the satellite line; that is, a change in width without change in qualitative shape.

5.4 Broadening from Hyperfine Structure[21,44,83]

The electrons associated with colour centres spread over atoms adjacent to the centre, and the hyperfine

interaction of these defect electrons with the nuclei of the neighbours broadens the spin resonance lines of the defect. For relatively compact centres, such as the F centre in alkali halides, the lattice must be treated as discrete. When this is coupled with the practical difficulty of calculating ρJ_c of (5.2), it can be seen that the statistical method is not very helpful. The moment method proves to be a useful substitute.[83,84]

The transition energy in EPR is

$$\hbar\omega=\hbar\omega_0+\sum_i a_i I_{zi}, \tag{5.5}$$

where $\mathbf{I}_i$ is the spin of the ith nucleus and a_i is a hyperfine coupling constant which can be measured in a separate ENDOR experiment, for example. The sum is over all nuclei in the crystal. Their distribution is known when the crystal structure near the defect is known. The second and fourth moments of the line shape can be found from (3.26) or (3.27); we follow Ref. 83 in using (3.27) since the line is symmetric when the temperature is appreciably larger than a_i/k. Then,

$$\langle\hbar^2(\omega-\omega_0)^2\rangle=\tfrac{1}{3}\sum_i a_i^2 I_i(I_i+1), \tag{5.6}$$

$$\langle\hbar^4(\omega-\omega_0)^4\rangle=\tfrac{1}{5}\sum_i a_i^4 I_i(I_i+1)[I_i(I_i+1)-\tfrac{1}{3}] +\tfrac{1}{3}\sum_{i>j}\sum_j a_i^2 a_j^2 I_i^2(I_i+1)^2. \tag{5.7}$$

Moments can only predict a linewidth, given a reasonable qualitative assumption about the shape. The assumption here is that the shape is Gaussian. It can be shown quite easily[9,16] that if the perturbations from all the N defects are of the same magnitude but of either sign, then the line shape tends to Gaussian in the limit of large N. This is an example of the central limit theorem.[85] For the hyperfine interaction all the nuclei in a shell of atoms around the centre have the same a_i and have I_{zi} which are positive and negative with equal probability. The number of atoms in each shell (of order 10) is large enough to make the assumption of a Gaussian plausible. The envelope of the EPR line is thus Gaussian of width

$$(\tfrac{2}{3}\ln 2)^{1/2}[\sum_i a_i^2 I_i(I_i+1)]^{1/2}. \tag{5.8}$$

We can make drastic assumptions and calculate the continuum result corresponding to (5.8). This is particularly useful in estimating the effect of summing over only a few shells in (5.8) and ignoring nuclei in more distant shells. As an approximation we assume that $a_i I_{zi}$ of (5.5) is replaced by

$$\epsilon(z_i)=A\exp(-\alpha r_i), \tag{5.9}$$

as the defect-electron wave function falls off roughly exponentially. Ignoring the interaction with shells inside a radius R and assuming a Gaussian shape, the width due to these distant nuclei alone is Δ_G, where

$$\Delta_G^2=2\ln 2(4\pi\rho A^2)\int_R^\infty dr r^2\exp(-2\alpha r); \tag{5.10}$$

ρ is the number of nuclei per unit volume. Alternatively, we may use the approximate method of Sec. 3.2. This makes no assumptions (or predictions) about the shape. In the limit where the linewidth Δ_A is appreciably larger than $A\exp(-\alpha R)$, the function $F(u)$ of (3.28) tends to 3. This limit is approached for widespread wave functions (α small) and large R. Equation (3.28) yields

$$\Delta_A^2=3(4\pi\rho A^2)\int_R^\infty dr r^2\exp(-2\alpha r), \tag{5.11}$$

so that $\Delta_A\simeq 1.47\Delta_G$. The agreement between Δ_A and Δ_G improves when (3.28) is solved graphically. When the nuclei inside R are the only ones considered, discrete lines result. The nuclei outside R broaden these discrete lines by about Δ_A. This additional broadening is negligible if Δ_A is appreciably less than (5.8), which gives the spread of the component lines due to the nuclei within the "discrete" region.

6. COMPARISON WITH EXPERIMENT

In the previous sections it has been shown that the shapes of inhomogeneous resonance lines can be calculated in terms of various properties of the defects causing broadening and of the centre whose transitions are observed. Thus, one needs to know the defect perturbation field $\epsilon(z)$, the defect concentration ρ, and the distribution of these defects with respect to the centres observed. Similarly, the coupling coefficients [the $\hbar\omega_1 a_{ij}$ of (3.1) and the $\hbar\omega_1\alpha_j$ of (3.2)] must be known, and one must be able to separate the inhomogeneous broadening from any other contributions present. Ideally, one would like to measure the defect distribution and concentration in the crystals for which the line shapes were measured. This ideal is rarely achieved. In other cases one has to be content with concentrations obtained from different specimens or from the starting material used to grow the crystals, and it is usual to resort to a continuum approximation for the distribution.

The various mechanisms will be discussed in the same order as in Secs. 4 and 5. Thus, we treat strain broadening by dislocations and by point defects and broadening by random electric field gradients, random electric fields, and by hyperfine interaction. No attempt is made to describe all experiments on inhomogeneous broadening; the experiments described are those for which the most detailed comparison of theory and experiment is possible.

6.1 Strain Broadening by Dislocations

This is one of the most common examples of inhomogeneous broadening, simply because of the practical

TABLE II. Full widths at half-intensity of strain distributions calculated from spin resonance data for ions in MgO. The strains are in units of 10^{-4}. ϵ_{001} is $2e_{zz}-e_{xx}-e_{yy}$ and ϵ_{111} is $e_{xy}+e_{yz}+e_{zx}$, where we do not use engineering notations. The references given are Refs. 89 (a)–(h).

Ion	Ref.	ϵ_{001}	ϵ_{111}	$\epsilon_{001}/\epsilon_{111}$
Cr^{3+}	a	1.7		
Mn^{2+}	b	1.8		
	c	2.0	0.64	3.1
Fe^{3+}	c	2.1	0.53	4.0
Fe^{2+}	d	2.0	0.60	3.2
	b	1.7	0.69	2.5
Fe^{1+}	e	1.5		
Co^{2+}	f	2.3		
	g(ENDOR)	2.8	2.8	1.0
Ni^{2+}	h	2.0	0.64	3.1
Theory	16	0.7	0.3	2.3

difficulty of growing crystals with low dislocation densities. The optical, EPR, and ENDOR properties of MgO doped with transition-metal ions provide comprehensive data for comparison with theory. We concentrate on the spin-resonance data, since the form of $\epsilon=\sum_{ij} a_{ij}e_{ij}$ depends on only the direction of the magnetic field for ions in cubic sites, and data from different ionic species may be compared. When the field is along the [001] axis, ϵ is $\epsilon_{001}=2e_{zz}-e_{xx}-e_{yy}$; when the field is along the [111] axis, ϵ is $e_{xy}+e_{yz}+e_{zx}\equiv\epsilon_{111}$. As the coupling coefficients $\hbar\omega_1$ are known from other experiments,[35,46,50,86–88] the observed spin resonance linewidths can be used to give the full widths at half-intensity of the distributions of ϵ_{001} and ϵ_{111}. These are given in Table II[16,89]; the differences arise partly from the analysis of the data (for example, it is often hard to subtract off the dipolar contribution to the width) and partly from differences in the defect content of the specimens. All the data have been analysed by the present author to ensure common notation.

For dislocations the strength of a defect is the length of the Burgers vector. This is mainly determined by the crystal structure; for MgO the Burgers vectors are oriented along ⟨110⟩ directions; their length is $\sqrt{2}a$, where $a=2.104$ Å is the nearest-neighbor distance. Lang and Miuscov[90] have studied the dislocation structure of MgO. They find the dislocation distribution to be markedly inhomogeneous with the dislocations concentrated into polygonal cell walls within individual subgrains. The precise structure depended on the source of the crystals and thus on their mechanical and thermal history. The total dislocation content in one particularly good crystal was estimated to be 2.5×10^5 cm/cc.

Any comparison of the continuum theory Sec. (4) with data for MgO must note some important differences. In the real crystal the dislocations are not straight nor are they distributed homogeneously. Furthermore, the distribution of the magnetic ions with respect to the dislocations is not known; any tendency to congregate near the dislocations is omitted in the theory. These differences will lead to differences between the predicted and observed line shapes. In addition, the crystals used in the experiments from which the results in Table II were culled may have been appreciably poorer than those used by Lang and Miuscov. We will adopt a dislocation density $L=5\times10^5$ cm/cc to take some account of the greater imperfection.

The observed shapes of the $I(\epsilon)$ are nearly Lorentzian,[34,88] although there is some dependence on the component of strain studied.[88] Thus, the observed $I(\epsilon_{001})$ appears to be remarkably Lorentzian, whereas $I(\epsilon_{111})$ shows a slight tendency to Gaussian, being narrower in the wings. The predicted shapes in both cases are nearly Gaussian, being given by Eq. (4.13). The difference between the predicted and observed shapes is attributed to the assumption of a homogeneous dislocation distribution. This view is supported by the zero phonon line shapes of colour centres in NaCl, as these (described later in Sec. 6.2) are nearly Gaussian when broadened by dislocations. The simple continuum theory does, however, predict the change of line shape with strain component correctly. The ratio of A and B of (4.13) depends on the form of $\psi(\theta, \phi, \alpha)$, and this, in turn, depends on the component of strain considered. The ratio varies within quite narrow limits and predicts that the line shape $I(\epsilon_{111})$ should be narrower in the wings than $I(\epsilon_{001})$.[88]

The calculated widths for ϵ_{001} and ϵ_{111} are 0.7×10^{-4} and 0.3×10^{-4} respectively, for a dislocation density of 5×10^5 cm/cc. For MgO:Fe^{2+} these would correspond to linewidths of 250 and 175 G at X band. Although these are of the right order of magnitude, they are rather less than the observed widths of about 600 and 350 G. To give the same half-widths, a dislocation density L of about 3×10^6 cm/cc would be needed, as the linewidth varies roughly as $L^{1/2}$. This is about an order of magnitude larger than the estimate of Ref. 90. Part (and possibly most) of the discrepancy can be attributed to the neglect of the subgrain structure, which is also responsible for the differences of the observed and calculated line shapes. The remaining differences in width reflect a higher dislocation density in the crystals used than in the crystals of relatively high perfection studied in Ref. 90.

The ratio of the widths, $\epsilon_{001}/\epsilon_{111}$, is predicted to be 2.3. This is within the rather broad limits set by experiment. This verifies, very crudely, the assumption of ⟨110⟩ Burger's vectors and isotropically distributed dislocation axes.

In summary, the line *shape* is not predicted well; on the other hand, the predicted variation of the shape and width with the magnetic field direction and the magnitude of the width agree well with experiment. The discrepancies can probably be attributed to the

complexity of the real dislocation structure as compared with the simple model assumed.

6.2 Strain Broadening by Point Defects

The defects considered here are elastic misfits but have the same charge as the ions they replace. Thus, only the "size" effect is important. The best examples are given by the mixed alkali halide systems, for example $NaCl_{1-x}Br_x$. These systems were used in early NMR experiments,[91] although the particular parameters of those experiments are not suitable for an accurate quantitative test of the theory. More recent experiments have shown the effect of strain broadening on the zero-phonon line of the N_1 centre in NaCl.[92] The results are described here.

The defect concentrations in mixed crystals were in the range 0.1–1.0 mole % and were measured chemically. The strengths of the defects are found from the change in lattice parameter per defect (the details are given in Appendix V). Since the concentrations were low and neither the colour centres studied nor the defects themselves are charge misfits, it is reasonable to assume that both are randomly distributed, and the line shapes observed seem to confirm this. The only remaining parameters needed are the coupling coefficients of the colour centres to the local strain. These were found in separate experiments in which external uniaxial stresses were applied.[93]

The experiments used NaCl crystals doped with one of the following ions: Li^+, K^+, F^-, Br^-, or I^-. The only real differences between the different dopings arose from the different strengths of the various defects. There were also some differences in the satellite lines.

The predicted line shape was confirmed. At low defect concentrations the zero-phonon line is strain broadened by dislocations and is nearly Gaussian in shape. As the point-defect concentration is increased the line becomes progressively Lorentzian. The agreement of the observed line shape with theory and the fact that the chemical nature of the defects is unimportant both tend to confirm that the defects and colour centre are distributed at random.

The line shift, the point-defect contribution to the linewidth, the fractional change in x-ray lattice parameter, and the concentration should all be related linearly. This is observed. The ratio of shift and width does not depend on the defect strength nor on the absolute magnitude of the coupling coefficients. It does, however, depend on Poisson's ratio ν. This is not uniquely defined for cubic crystals, although there are fairly severe limits (for NaCl $0.167 \leq \nu \leq 0.363$). The value $\nu = 0.2$ gives best agreement with experiment, although it is smaller than the Voigt value of 0.238. The same choice of ν works equally well for all the chemically different species of defect. With this choice of ν, roughly 87% of the shift comes from the Eshelby term in (4.23). The ratio of shift to change in lattice parameter depends on the coupling coefficients $\hbar\omega_1 a_{ij}$ but not on the strengths of the defects. There is a discrepancy here as the ratio of shift to lattice parameter change is some 30% more than predicted. Up to half this difference may come from errors in the coupling coefficients; the remainder is not yet understood. Possibly, the rest comes from the effects of anisotropy or from differences in the displacements of the anions and cation lattices.[106]

The defects also introduce satellite lines. These satellites appear to have the same shape as the main line (consistent with the predictions of Sec. 5.2) but it is difficult to establish the exact atomic configurations which give rise to them.

6.3 Broadening by Random Field Gradients

Point defects can be charge misfits as well as elastic misfits. Because centres sensitive to strains are also sensitive to field gradients, the charge itself can cause broadening. When both electrostatic and elastic effects are important, the results may be hard to interpret, as was discussed in Sec. 4.3. Here we consider the "charge" effect rather than the "size" effect.

No case of a charge misfit which is not an elastic misfit seems to be given in the literature. The closest appears to be $MgO:Er^{3+}$, where Er^{3+} has an ionic radius some 35% larger than that of the Mg^{2+} it replaces.[94] Even here the "size" and "charge" effects should be comparable. In this system, random field gradients appear to broaden the EPR line.[18] The Er^{3+} is both the centre whose transitions are studied and also one of the defects responsible for the broadening.

In Ref. 18 the defect concentration was estimated from the degree of doping of the MgO and was checked later by direct measurement. The coupling coefficients were not measured but estimated theoretically. These calculations are very similar in nature to the calculations of spin–lattice coupling coefficients which have proved reliable in rough order of magnitude.[87] The theoretical values need a local field correction, as in Eq. (4.2).[61] In view of the approximations, including the neglect of other species present for charge compensation, the predicted and observed linewidths are in acceptable agreement. In addition the dependence of the width on magnetic field orientation is satisfactory. No attempt was made to check the concentration dependence of the width or to subtract off the contribution of the dislocation strain broadening.

The line shape observed was nearly Lorentzian. This agrees with the predicted shape, although it should be noted that other mechanisms which may have been important make the same prediction (notably strain broadening by point defects and, possibly, by dislocations in subgrain boundaries).

6.4 Broadening by Random Electric Fields

This is only important when the centres studied are at sites which lack inversion symmetry. The shift in

TABLE III. A comparison of F-center linewidths observed and predicted. The table is taken in part from Ref. 44; Refs. 97 (a)–(d) gives the original references.

Crystal	Measured width (gauss)		Predicted width (gauss)
LiCl	68	a	90
NaCl	165	a, b	190
NaBr	353	a	240
RbBr	450 (natural)	c	360(^{85}Rb), 750(^{87}Rb)
RbI	750 (natural)	c	440(^{85}Rb), 790(^{87}Rb)
CsCl	800	d	1020

energy due to internal electric field is, of course, just the Stark effect of conventional spectroscopy.

Most of the work on this mechanism has been done on the tungstates doped with paramagnetic ions, in particular $CaWO_4$ containing Ce^{3+}, Er^{3+}, and Mn^{2+} (Ref. 15) and $ZnWO_4$:Cr^{3+}.[79] The magnetic ions substitute for the divalent cations and are at sites with S_4 point symmetry. The charged defects which cause the random electric fields are mainly the magnetic ions themselves (when they are not divalent), other ions which have been introduced for charge compensation, and the vacancies remaining after crystallisation from the melt. The concentrations of impurity ions can be measured chemically.[15] It is harder to obtain the concentration of intrinsic defects, although data taken near the melting point of $CaWO_4$ are available[95] and provide an upper limit to the vacancy concentration. The coupling coefficients [the α_j of Eq. (3.2)] are found by observing the shift of the resonance line under an external applied electric field.[51] The strengths of the defects are known in terms of their charge and of the host-crystal dielectric constant.

Experiment and theory are in accord. The line shapes observed are intermediate between Gaussian and Lorentzian. The shapes observed in Ref. 15 were close to the Holtsmark shape predicted, whereas those of Ref. 79 were between the Holtsmark and Lorentz shapes. The enhanced intensity in the wings found in Ref. 79 may be due to correlation between the Cr^{3+} ions and the Li^+ added for charge compensation. Satellite lines have been detected due to defects close to magnetic ions,[79] but it has not proved possible to sort out the detailed configurations concerned. The predicted widths agree reasonably with those observed. For example, in $ZnWO_4$:Cr^{3+} charge compensated with Li^+, the predicted width at a Cr^{3+} concentration of 0.05% is 0.9×10^5 V/cm; the experimental width is 1.18×10^5 V/cm.[79] Similar agreement is reported in $CaWO_4$.[15] The width depends on the magnetic field direction and on the concentration of defects. The concentration dependence is confirmed approximately, being (concentration)$^{1/2}$ rather than the dependence (concentration)$^{2/3}$ expected.[79] The dependence on magnetic field orientation has also been verified.[15,79] This dependence was one of the first observations which suggested the resonance lines were inhomogeneously broadened by random electric fields (see Sec. 2).

6.5 Broadening from Unresolved Hyperfine Structure

Electrons trapped at negative-ion vacancies in alkali halides (F centres) have spin resonance lines broadened by hyperfine interaction with the nuclei of the host lattice. The F centre wave function is fairly compact, so that the interaction is only important over a short range from the centre. As a result, continuum models are not really adequate, and it was necessary to recognise the discreteness of the lattice. However, semi-quantitative arguments can be given (Refs. 9, 16, 83; see also Sec. 5.3) suggesting a Gaussian line shape for which the width can be found from the second moment.

The distribution and concentration of the nuclei which cause the broadening are known in this case, as the lattice structure and isotopic abundances are known. Some allowance for local distortion of the lattice should be made, but this is rarely important for the linewidth. It is much harder to obtain the perturbation field $\epsilon(z)$. The only really satisfactory way is to resolve the hyperfine structure by ENDOR and to measure the parameters directly. A less satisfactory alternative is to use a purely theoretical estimate. When $\epsilon(z)$ is known, all the necessary data are available.

The observed lines are indeed Gaussian, and it can be seen from Table III that the widths are given with reasonable accuracy.

7. CONCLUSION

In this review the most fruitful method of calculating inhomogeneous line shapes has been the statistical method. Other approaches, particularly the moment method, are sometimes useful. The predictions have been compared with experiment for a number of broadening mechanisms with satisfactory agreement. The discrepancies are often the result of incomplete experimental data; there is a strong case for checking the theory by further experiments in which all the important parameters are measured.

The theory also predicts the relative magnitudes of the various inhomogeneous mechanisms (see especially Sec. 4.6). When the mechanism is known the observed shapes and widths can be used in several ways. First, some information can be obtained about the distribution of the centres studied relative to the defects. Thus the relative distribution of two different types of centre can be compared, at least qualitatively, to see if one centre is more strongly correlated with the defects than the other. In principle, the distribution function $p(z)$ can be obtained from the line shape, but the practical difficulties of inverting the fundamental equations [(3.13), (3.19), and (3.20)] with an experimentally determined $I(\epsilon)$ are immense. Second, one can compare the response of different centres of the internal perturbation field. If they are assumed to experience the same distribution of perturbations, then the widths

of the resonance lines in the two cases gives a measure of the coupling coefficients ($\hbar\omega_1 a_{ij}$ or $\hbar\omega_1\alpha_j$ in our earlier notation) of these centres. This can be done for strains in the lattice (see, for example, Ref. 88) and should be even more useful for random electric fields. In the case of broadening of electric fields, the coupling coefficients should tell if the centre involved has inversion symmetry and thus distinguish between various models of the centre. Third, one can obtain an estimate of the strength of the defects responsible for the broadening, for example the A_k for point defects described in (4.17). This may prove useful when several species of point defect are involved, for the linewidth depends only on the magnitudes $|A_k|$ of the strengths. Other measurements, such as the fractional change in x-ray lattice parameter or in macroscopic length, depend on the relative signs of the A_k for the various defects; the cancellation between the effects of defects with opposite sign strengths makes analysis of these cases difficult.

The problems remaining lie in more complicated situations. The treatment of cases where second-order effects are important is still incomplete. Also, more realistic models than the continuum approximation of Sec. 4 are needed; one example would be to take account of the subgrain structure in crystals with dislocations. It remains to be seen if the statistical method is as fruitful in these situations.

ACKNOWLEDGMENTS

The author wishes to thank Dr. A. B. Lidiard, Dr. R. Bullough, and Dr. A. E. Hughes for helpful discussions, Dr. J. D. Eshelby for helpful correspondence and Dr. E. Belorizky, Dr. M. F. Lewis, Dr. W. S. Moore, Dr. K. A. Müller, Dr. P. E. Wagner, and Dr. R. F. Wentzel for details of their work prior to publication.

APPENDIX I: STRAIN BROADENING BY DISLOCATIONS

Here we calculate $J(x)$ and $I(\epsilon)$. $J(x)$ is

$$\sum_i F_i \int_0^\pi d\theta \sin\theta \int_0^{2\pi} d\phi \int_0^{2\pi} d\alpha \int_{R_1}^{R_2} dr r \times\{1-\exp[-ix(b/\pi r)\psi]\}. \quad \text{(A1.1)}$$

We concentrate on the inner integral. Its real part is

$$\int_{R_1}^{R_2} dr r\left[1-\cos\left(x\frac{b}{\pi r}\psi\right)\right]=R_2^2\int_{R_1/R_2}^1 dv v\left(1-\cos\frac{u}{v}\right) =\tfrac{1}{2}R_2^2u^2\{f(u)-f[u(R_2/R_1)]\}, \quad \text{(A1.2)}$$

where $v=r/R_2$, $u=x(b/\pi R_2)\psi$, and

$$f(t)=[(1-\cos t)/t^2]+[(\sin t)/t]-\mathrm{Ci}(t).$$

$\mathrm{Ci}(t)$ is the cosine integral of Jahnke and Emde.[98] It is straightforward to show that $R_1=0$ is a good approximation. Using the asymptotic form of $\mathrm{Ci}(t)$ for small t (A1.2) becomes $\frac{1}{2}R_2^2u^2[0.9228+\ln(1/|u|)]$. Combining this with (A1.1) we obtain (4.11 and 4.12).

In practice the integrals

$$I_2=\sum_i F_i\int_0^\pi d\theta\sin\theta\int_0^{2\pi}d\phi\int_0^{2\pi}d\alpha\,|\psi|^2,$$

$$I_3=\sum_i F_i\int_0^\pi d\theta\sin\theta\int_0^{2\pi}d\phi\int_0^{2\pi}d\alpha\,|\psi|^2\ln|\psi|$$

are obtained by numerical integration.

The imaginary part of the inner integral in (A1.1) is

$$\int_{R_1}^{R_2} dr r\sin\left(x\frac{b}{\pi r}\psi\right)=R_2^2\int_{R_1/R_2}^1 dv v\sin(u/v) =\tfrac{1}{2}R_2^2u^2\{f'(u)-f'[u(R_2/R_1)]\},$$

in which

$$f'(t)=\mathrm{Si}(t)+(\sin t/t^2)+(\cos t/t).$$

$\mathrm{Si}(t)$ is the sine integral of Jahnke and Emde. Again $R_1=0$ is a good approximation, and with the asymptotic form of $\mathrm{Si}(t)$ we obtain (4.15).

APPENDIX II: BROADENING BY DISLOCATION DIPOLES

For simplicity of notation we abbreviate $(\theta, \phi, \alpha, \beta, \mathbf{b}_i/|b|)$ by Ω and denote the corresponding sums and integrals over these variables by $\int d\Omega$. $J(x)$ is given by (3.22), where $p(z)\,dz\sim r\,dr$ and $\epsilon(z)\sim bl\psi(\Omega)/r^2$. Thus,

$$J(x)=\int d\Omega\int_{R_1}^{R_2} dr r\{1-\cos[xbl\psi(\Omega)r^{-2}]\}.$$

The substitution $y=|[xbl\psi(\Omega)]/r^2|$ simplifies this. Making the further approximations $R_1\to 0$ and $R_2\to\infty$, we have

$$J(x)=\frac{1}{2}\int d\Omega\,|xbl\psi(\Omega)|\int_0^\infty dy\frac{1-\cos y}{y^2}$$

$$=\tfrac{1}{4}\pi|x|bl\int d\Omega\,|\psi|.$$

Recalling that $\rho=L/8\pi^2$ for dipoles, the result of Sec. 4.2 is obtained.

APPENDIX III: STRAIN BROADENING BY POINT DEFECTS

Here we calculate

$$\rho J(x)=\rho\int d\Omega\int_{R_1}^{R_2} dr r^2\left[1-\exp\left(-iA\psi\frac{x}{r^3}\right)\right]$$

$$=\rho\int d\Omega\int_{R_1}^{R_2} dr r^2\left[1-\cos\left(A\psi\frac{x}{r^3}\right)\right] +i\rho\int d\Omega\int_{R_1}^{R_2} dr r^2\sin\left(A\psi\frac{x}{r^3}\right). \quad \text{(A3.1)}$$

The integral over Ω is simply an integral over angles:

$$\int d\Omega\equiv\int_0^\pi d\theta\sin\theta\int_0^{2\pi}d\phi.$$

The substitutions $y=1/r^3$, $Y=1/R_1^3$, and $B=A\Psi x$ reduce (A3.1) to the form

$$J(x)=\frac{1}{3}\int d\Omega\int_{1/R_2^3}^{Y}dy\,\frac{1-\cos By}{y^2}+\tfrac{1}{3}i\int d\Omega\int_{1/R_2^3}^{Y}dy\,\frac{\sin By}{y^2}. \quad \text{(A3.2)}$$

The first term [the real part of $J(x)$] presents no difficulties in the limit $R_2\to\infty$, that is, for an unlimitedly large crystal. Direct integration yields

$$\mathrm{Re}\,[J(x)]=\tfrac{1}{3}(\,|\,A\,||\,x\,|\,)\int d\Omega\,|\,\psi\,|\,\mathrm{Si}\left(\left|A\psi\frac{x}{R_1^3}\right|\right)+\tfrac{1}{3}R_1^3\int d\Omega\cos\left(A\psi\frac{x}{R_1^3}\right)-\tfrac{4}{3}\pi R_1^3. \quad \text{(A3.3)}$$

Si (x) is the sine integral of Ref. 98. Re (J) is also finite when $R_1\to 0$ when

$$\mathrm{Re}\,J(x)=\tfrac{1}{6}\pi\,|\,A\,||\,x\,|\left(\int d\Omega\,|\,\psi\,|\,\right). \quad \text{(A3.4)}$$

This result has been used in (4.21).

The second term in (A3.2) must be solved more carefully, keeping R_1 and R_2 finite. Direct integration prior to taking the limit $R_2\to\infty$ yields

$$-\mathrm{Im}\,J(x)=\tfrac{1}{3}R_1^3\int d\Omega\sin\left(A\psi\frac{x}{R_1^3}\right)-\tfrac{1}{3}(xA)\int d\Omega\psi\,\mathrm{Ci}\left(\left|A\psi\frac{x}{R_1^3}\right|\right)+\lim_{R_2\to\infty}xA\int d\Omega\,\psi\,\mathrm{Ci}\left(\left|A\psi\frac{x}{R_2^3}\right|\right). \quad \text{(A3.5)}$$

We now use the asymptotic form of the cosine integral

$$\lim_{u\to 0}\mathrm{Ci}\,(\,|\,u\,|\,)=\ln\gamma+\ln|\,u\,|,$$

where γ is Euler's constant. The condition

$$\int d\Omega\psi=0 \quad \text{(A3.6)}$$

is valid for all ψ_{ij}, where

$$\psi_{ij}=\delta_{ij}-(3x_ix_j/r^2); \quad \text{(A3.7)}$$

the zero angular integral is able to ensure convergence of (A3.5).* On reduction we obtain

$$-\mathrm{Im}\,[J(x)]=\tfrac{1}{3}Ax\int d\Omega\psi\ln|\,\psi\,|+\tfrac{1}{3}R_1^3\int d\Omega\sin\left(Ax\frac{\psi}{R_1^3}\right)-\tfrac{1}{3}Ax\int d\Omega\psi\,\mathrm{Ci}\left(\left|Ax\frac{\psi}{R_1^3}\right|\right). \quad \text{(A3.8)}$$

In the limit $R_1\to 0$ we obtain the result used in (4.21):

$$-\mathrm{Im}\,J(x)=\tfrac{1}{3}Ax\int d\Omega\psi\ln|\,\psi\,|.$$

The over-all form of $\rho J(x)$ in the limits of $R_1=0$, $R_2=\infty$ is

$$\rho J(x)=\left(\tfrac{1}{6}\pi\,|\,A\,|\int d\Omega\,|\,\psi\,|\,\right)|\,x\,|-i\left(\tfrac{1}{3}A\int d\Omega\psi\ln|\,\psi\,|\,\right)x=\alpha_R\,|\,x\,|-i\alpha_I x.$$

$I(\epsilon)$ is given by

$$I(\epsilon)=\frac{1}{2\pi}\int_{-\infty}^{\infty}dx\exp(ix\epsilon)\exp(-\alpha_R\,|\,x\,|\,)\exp(i\alpha_I x),$$

which is a Lorentzian of width $2\alpha_R$ centred on $\epsilon=-\alpha_I$.

APPENDIX IV: BROADENING BY RANDOM ELECTRIC FIELDS

Here we find $I(\epsilon)$ and $\rho J(x)$. By (4.25) and (4.26)

$$\rho J(x)=\rho\int_0^{2\pi}d\phi\int_0^{\pi}d\theta\sin\theta\int_{R_1}^{R_2}drr^2\times\left[1-\exp\left(\frac{ixZ\cos\theta}{r^2}\right)\right]$$

$$=\rho\int_0^{2\pi}d\phi\int_0^{\pi}d\theta\sin\theta\int_{R_1}^{R_2}drr^2\times\left[1-\cos\left(\frac{xZ\cos\theta}{r^2}\right)\right]-i\rho\int_0^{2\pi}d\phi\int_{R_1}^{R_2}drr^2\int_{-1}^{1}d(\cos\theta)\sin\left(\frac{xZ\cos\theta}{r^2}\right).$$

The second integral vanishes since its integrand is an odd function of $\cos\theta$. This means that the resonance line is not shifted and is a direct result of our assumption of an *isotropic* continuum.

We let $R_2\to\infty$ (the large crystal limit) and introduce $u=\cos\theta$ and $v=1/r^2$:

$$\rho J(X)=\rho\frac{1}{2}\int_0^{2\pi}d\phi\int_{-1}^{1}du\int_0^{1/R_1{}^2}dv\,\frac{1-\cos(Zxuv)}{v^{5/2}}=2\pi\rho\,|\,Z\,|^{3/2}\,|\,x\,|^{3/2}\int_0^{|Z||x|/R_1{}^2}dw\,\frac{w-\sin w}{w^{7/2}}.$$

The innermost integral can be evaluated in terms of the integral

$$C(a)=\int_1^{\infty}dz\,\frac{\cos(az)}{Z^{1/2}},$$

* For a more detailed discussion in the special case $\Psi\equiv\Psi_{zz}$, see the Appendix to Grant and Strandberg's paper.[14]

related to the Fresnel integrals of Ref. 99. Finally

$$\rho J(x)=\tfrac{4}{15}(2\pi)^{3/2}\rho\,|\,Z\,|^{3/2}\,|\,x\,|^{3/2}-\tfrac{4}{3}\pi R_1{}^3\rho$$
$$+\tfrac{16}{15}\pi\rho\,|\,Z\,|^{3/2}\,|\,x\,|^{3/2}[\tfrac{3}{4}(\sin X/X^{5/2})+\tfrac{1}{2}(\cos X/X^{3/2})$$
$$-(\sin X/X^{1/2})-X^{1/2}C(X)\,].$$

X is $|\,Zx/R_1{}^2\,|$. In the limit $R_1\to 0$, only the first term remains; this has been used to obtain (4.28).

APPENDIX V: STRENGTHS OF POINT DEFECTS

The long-range displacement field around a point defect in an isotropic lattice is $A(\mathbf{r}/r^3)$, where A is the defect strength. Measurements of these strengths are rather isolated in the literature, so a number of useful results are collected here.

Occasionally the strengths are given explicitly. Thus, Ref. 100 gives $A=1.4\pm0.3$ Å^3 for B in silicon. More usually $\Delta V/V$, the fractional change in volume per defect, is given. This is related to the strength by

$$A=[(1+\nu)/12\pi(1-\nu)\,]\,\Delta V,$$

where ν is Poisson's ratio. These results assume isotropic elasticity theory, so for cubic crystals the Voigt average of ν is used,[72c] viz.,

$$\nu=\tfrac{1}{2}[(4c_{12}-2c_{44}+c_{11})/(3c_{12}+c_{44}+2c_{11})\,].$$

As an explicit example for a mixed crystal of KBr containing a little KCl,

$$(\Delta V/V)\simeq 3(a_{\mathrm{KCl}}-a_{\mathrm{KBr}})/a_{\mathrm{KBr}}, \qquad \text{(A5.1)}$$

where a_x is the nearest-neighbour distance for pure crystal x. Then ρA, which appears in the expressions for the linewidth and shift [Eqs. (4.21) and (4.23)] is

$$\rho A\simeq f_{\mathrm{Cl}}(4\pi)^{-1}\frac{1+\nu}{1-\nu}\frac{a_{\mathrm{KCl}}-a_{\mathrm{KBr}}}{a_{\mathrm{KBr}}}$$

in which f_{Cl} is the ratio of the numbers of Cl^- and Br^- ions.

In the list below, E and T denote experimental results and theoretical predictions, respectively:

Crystal	*Defect*	$\Delta V/V$	*Refs.*
MgO	O^{2-} vacancy	-0.4	E, 72b
	O^{2-} interstitial	$+3.0$	E, 72b
	F centre	$+0.075$	T, 101
Si	Vacancy	$+0.6$	T, 72a
	B substitutional	$+0.07$	E, 100
Ge	Vacancy	$+0.7$	T, 72a
KCl	*F* Centre	0.58 ± 0.3	E, 102
	F Centre	0.31	T, 103
	Ca^{2+} substitutional	-0.52 ± 0.05	E, 104
	Sr^{2+} substitutional	-0.13 ± 0.04	E, 104

The expression (A5.1) assumes that the lattice parameter of mixed alkali halides changes linearly with concentration at all concentrations. Such formulae must be used with caution. In particular they are usually invalid when solid solutions of the two species cannot be found in any concentration ratio.[105]

REFERENCES

[1] A. A. Markoff, *Wahrscheinlichkeitsrechnung* (Teubner, Leipzig, 1912) (described in Ref. 7).
[2] J. Holtsmark, Ann. Physik **58,** 577 (1919); Physik. Z. **20,** 162 (1919); **25,** 73 (1924).
[3] H. Margenau, Phys. Rev. **48,** 755 (1935).
[4] H. Margenau and J. Watson, Rev. Mod. Phys. **8,** 22 (1936).
[5] H. Margenau, Phys. Rev. **82,** 156 (1951).
[6] H. Margenau and M. Lewis, Rev. Mod. Phys. **31,** 569 (1959).
[7] S. Chandrasekhar, Rev. Mod. Phys. **15,** 1 (1943).
[8] P. W. Anderson, Phys. Rev. **82,** 342 (1951).
[9] M. H. Cohen and F. Reif, Solid State Phys. **5,** 322 (1955).
[10] R. G. Breene, Rev. Mod. Phys. **29,** 94 (1957).
[11] A. Abragam, *The Principles of Nuclear Magnetism* (Oxford University Press, London, 1961).
[12] G. Ecker, Z. Physik **148,** 593 (1957).
[13] W. J. C. Grant, Phys. Rev. **134,** A1554, A1565, A1574 (1964); **135,** A1265 (1964).
[14] W. J. C. Grant and M. W. P. Strandberg, Phys. Rev. **135,** A715, A727 (1964).
[15] W. B. Mims and R. Gillen, Phys. Rev. **148,** 438 (1966).
[16] A. M. Stoneham, Proc. Phys. Soc. (London) **89,** 909 (1966).
[17] A. M. Stoneham, Proc. Colloq. AMPERE (At. Mol. Etudes Radio Elec.) 14th Ljubljana, 1966, 853 (1968).
[18] Y. Ayant and E. Belorizky, J. Phys. (Paris) **27,** 24 (1966); E. Belorizky, thesis, Université de Grenoble, 1966.
[19] I. M. Dubrovskiy, Phys. Metals Metallogr. (USSR) (English Transl.) **21,** 10 (1966).
[20] B. A. Greenberg, Phys. Status Solidi **17,** 673 (1966).
[21] V. Ya. Zevin, Zh. Eksp. Teor. Fiz. **5a,** 431 (1966) [Sov. Phys.—JETP **23,** 287 (1966)].
[22] A. M. Portis, Phys. Rev. **91,** 1071 (1953).
[23] Some nuclear physicists contend that "linewidth" can only mean the contribution of the finite lifetime to the width. I do not accept this. In the present article "linewidth" means the observed width of the resonance line.
[24] W. J. Brya and P. E. Wagner, Phys. Rev. **157,** 400 (1967).
[24a] The terms "phonon bottleneck" and "phonon avalanche" are defined in Ref. 24. They describe spin–lattice relaxation phenomena in cases where the rate-determining process is some process in the phonon system, rather than the transfer of energy from the spin system to the lattice.
[25] R. Kubo and K. Tomita, J. Phys. Soc. Japan **9,** 888 (1954).
[26] R. Kubo, *Fluctuation, Relaxation and Resonance in Magnetic Systems,* D. ter Haar, Ed. (Oliver and Boyd, Edinburgh, 1961), p. 23.
[27] J. H. Van Vleck, Phys. Rev. **74,** 1168 (1948).
[28] W. J. C. Grant, Physica **30,** 1433 (1964).
[29] M. Lax, J. Chem. Phys. **20,** 1752 (1952).
[30] D. Shaltiel and W. Low, Phys. Rev. **124,** 1062 (1961). (a) See M. Lax (Ref. 29) and J. J. Markham, Rev. Mod. Phys. **31,** 956 (1959); M. H. L. Pryce, in *Phonons in Perfect Lattices and in Lattices with Point Imperfections,* R. W. H. Stevenson, Ed. (Oliver and Boyd, London, 1965), p. 403. A. A. Maradudin, Solid State Phys. **18,** 274 (1966); **19,** 2 (1966). (b) General references are Kubo and Tomita (Refs. 25, 26) and Abragam (Ref. 11). For NMR, C. D. Jeffries, *Dynamic Nuclear Reorientation* (Interscience Publishers, Inc., New York, 1963), V. Jaccarino, *Magnetism IIA,* G. Rado and H. Suhl, Eds. (Academic Press Inc., New York, 1965). For EPR in paramagnetic insulators, A. A. Manenkov and R. Orbach, *Spin Lattice Relaxation in Solids* (Harper and Row, Publishers, Inc., New York, 1966); K. W. H. Stevens, Rept. Progr. Phys. **30,** 189 (1967). For magnetic materials, C. W. Haas and H. B. Callen, *Magnetism I,* G. Rado and H. Suhl, Eds. (Academic Press Inc., New York, 1963); J. H. van Vleck, J. Appl. Phys. **35,** 882 (1964); M. Sparks, *Ferromagnetic Relaxation Theory* (McGraw-Hill Book Co., New York, 1965). (c) Dipolar and exchange interactions are discussed by Van Vleck (Ref. 27), by Grant and Strandberg (Ref. 14), and by P. W. Anderson and P. R. Weiss, Rev. Mod. Phys. **25,** 269 (1953).
[31] N. Bloembergen and T. T. Rowland, Acta. Met. **1,** 731 (1953). T. J. Rowland, *ibid.* **3,** 74 (1955).

[32] F. Reif, Phys. Rev. **100,** 1597 (1955).
[33] R. D. King and B. Henderson, Proc. Phys. Soc. (London) **89,** 153 (1966). The nature of zero phonon lines is discussed in the review by A. A. Maradudin, Solid State Phys. **18,** 274; **19,** 2 (1966).
[34] D. McMahon, Phys. Rev. **134,** A128 (1964).
[35] E. Feher, Phys. Rev. **136,** A145 (1964).
[36] A. M. Stoneham (unpublished work, 1964).
[37] A. L. Schawlow, *Advances in Quantum Electronics III*, P. Grivet and N. Bloembergen, Eds. (Columbia University Press, New York, 1963).
[38] D. E. Eastman, R. J. Joenk, and D. T. Teaney, Phys. Rev. Letters **17,** 300 (1966).
[39] C. Kittel and E. Abrahams, Phys. Rev. **90,** 238 (1953).
[40a] G. Feher, Phys. Rev. **114,** 1219 (1959).
[40b] M. F. Lewis, Phys. Letters **17,** 183 (1965).
[41] R. Hilsch and R. W. Pohl, Z. Physik **64,** 606 (1930).
[42] P. R. Whittlestone, Ph.D. thesis, Bristol University, 1964 (unpublished).
[43] A. M. Portis, Phys. Rev. **91,** 1071 (1953).
[44] J. J. Markham, *F centres in Alkali Halides* (Academic Press Inc., New York, 1966), Sec. 21.
[45] L. D. Schearer and T. L. Estle, Solid State Commun. **4,** 639 (1966).
[46] K. A. Müller and W. Berlinger, Bull. Am. Phys. Soc. **12,** 40 (1967).
[47] A. M. Clogston, H. Suhl, L. R. Walker, and P. W. Anderson, J. Phys. Chem. Solids **1,** 129 (1956).
[48] S. Geschwind and A. M. Clogston, Phys. Rev. **108,** 49 (1957).
[49] A. M. Clogston, J. Appl. Phys. **29,** 334 (1958).
[50] G. D. Watkins and E. R. Feher, Bull. Am. Phys. Soc. **7,** 29 (1962).
[51] W. B. Mims, Phys. Rev. **140,** A541 (1965).
[52] A. A. Kaplyanskii, Opt. Spectrosk. **16,** 602 (1959) [Opt. Spectrosc. **7,** 409 (1959)]; (a) **16,** 602 (1964) [**16,** 329 (1964)]; (b) **16,** 1031 (1964) [**16,** 557 (1964)].
[53] W. A. Runciman, Proc. Phys. Soc. (London) **86,** 629 (1965).
[54] A. E. Hughes and W. A. Runciman, Proc. Phys. Soc. (London) **86,** 615 (1965); **90,** 827 (1967).
[55] P. L. Leath and B. Goodman, Phys. Rev. **148,** 968 (1966).
[56] P. Schofield, Brit. J. Appl. Phys. (to be published).
[57] A. M. Stoneham, J. Phys. (London) **C1,** 565 (1968).
[58] R. Bullough and R. C. Newman, Progr. Semiconductors **7,** 101 (1963).
[59] E. E. Salpeter, Ann. Phys. (Paris) **5,** 183 (1958).
[60] T. L. Hill, *Statistical Mechanics* (McGraw-Hill Book Co., New York, 1956).
[61] In Ref. 18 the numerical value of the optical constant is used in error, even though the text refers to the static constant.
[62] J. A. Stratton, *Electromagnetic Theory* (McGraw-Hill Book Co., New York, 1941).
[63] In Ref. 9 the results correspond to $\kappa_1=1$, $\kappa_2=\epsilon$, i.e. a polarizable region around each centre, but the rest of the lattice unpolarizable. The usual assumption is the converse, $\kappa_1=\epsilon$, $\kappa_2=1$.
[64] J. R. Hardy and A. B. Lidiard, Phil. Mag. **15,** 825 (1967).
[65] J. D. Eshelby, Solid State Phys. **3,** 79 (1956).
[66] We distinguish between the *expansion* which occurs in the absence of a free surface due to the singularities at the defects, and the uniform *dilatation* which appears when the surface tractions are made to vanish. In the absence of a surface the dilatation is zero except at the defect. Both terms contribute to the change of lattice parameter.
[67] R. W. Balluffi and R. O. Simmons, J. Appl. Phys. **31,** 2284 (1960).
[68] K. Fischer and H. Hahn, Z. Physik **172,** 172 (1963).
[69] For a linear effect the matrix element of the electric field connecting the two close states must exceed the difference in the (unperturbed) energies of the states. As the matrix elements will be of order $[|\mathbf{E}|(\mathrm{V/cm})\cdot 10^{-8}]$ eV the separation must be less than, say, 10 cm^{-1} for $|\mathbf{E}|\sim 10^5$ V/cm.
[70] Holtsmark actually calculated the probability that the *magnitude* of **E** lay in a particular range, irrespective of its direction. We have found the distribution of the *projection* of **E** on to the **b** direction.
[71] In Ref. 15 the integral after their equation (11) is in error. This introduces an extra factor 2 in (4.28).
[72] (a) A. Scholz and A. Seeger, Proc. Intern. Conf. Phys. Semicond. 7th, Paris, 1964, **3,** 315 (1965); (b) B. S. Hickman and D. G. Walker, Phil. Mag. **11,** 1101 (1965); D. H. Bowen, *The Nature of Small Defect Clusters*, M. J. Makin, Ed. (U.K.A.E.A. Report AERE-R. 5269, H. M. Stationery Office, London, 1966), p. 461; (c) W. Voigt, *Lehrbuch der Kristal Physik* (Teubner, Leipzig, 1928).
[73] J. R. Hardy, Phys. Chem. Solids **15,** 39 (1960).
[74] Y. Fukai, J. Phys. Soc. Japan **18,** 1580 (1963).
[75] A. Hartland, Proc. Roy. Soc. (London) **A304,** 361 (1968).
[76] L. O. Andersson, *Proceedings of the Conference on Point Defects in Non-Metallic Solids, Brighton, 1966* (J. Brit. Ceram. Soc., to be published); Helv. Phys. Acta. **40,** 364 (1967).
[77] J. Wertz and P. Auzins, Phys. Rev. **106,** 484 (1957).
[78] B. Henderson and T. P. P. Hall, Proc. Phys. Soc. (London) **90,** 511 (1967).
[79] W. S. Moore and J. Neal, British Radio Spectroscopy Conference, Redhill, 1966 (unpublished); B. F. Jones, W. S. Moore and J. Neal, J. Phys. (London) **D1,** 41 (1968).
[80] F. Seitz, Phys. Rev. **83,** 134 (1951).
[81] J. H. Schulman and W. D. Compton, *Colour Centres in Solids* (Pergamon Press, Inc., New York, 1962).
[82] G. F. Imbusch, A. Schawlow, A. D. May, and S. Sugano, Phys. Rev. **140,** A830 (1965).
[83] C. Kittel, *Defects in Crystalline Solids* (The Physical Society, London, 1954), p. 33.
[84] The treatment of Ref. 21, while set up as if using the statistical method, is essentially a treatment by the method of moments.
[85] M. F. Kendall and A. Stuart, *Advanced Theory of Statistics* (Griffin, London, 1958), Vol. 1.
[86] N. S. Shiren, Bull. Am. Phys. Soc. **7,** 29 (1962).
[87] E. B. Tucker, Proc. IEEE **53,** 1547 (1965).
[88] M. F. Lewis and A. M. Stoneham, Phys. Rev. **164,** 271 (1967).
[89] (a) J. G. Castle and D. W. Feldman, Phys. Rev. **121,** 1349 (1961); (b) D. McMahon, *ibid.* **134,** A128 (1964); (c) E. Feher, *ibid.* **136,** A145 (1964); (d) M. F. Lewis, Phys. Letters **19,** 459 (1965); (e) K. A. Müller and W. Berlinger, Bull. Am. Phys. Soc. **12,** 40 (1967); (f) P. R. Whittlestone, Ph.D. thesis, Bristol, (1964); (g) D. J. I. Fry and P. M. Llewellyn, Proc. Roy. Soc. (London) **A226,** 84 (1962); (h) M. F. Lewis and A. M. Stoneham, Phys. Rev. **164,** 271 (1967).
[90] A. R. Lang and V. F. Miuscov, Phil. Mag. **10,** 263 (1964).
[91] H. Kawamura, E. Otsuka, and K. Ishiwatari, J. Phys. Soc. Japan **11,** 1064 (1956).
[92] A. E. Hughes, J. Phys. Chem. Solids **29,** 1461 (1968).
[93] A. E. Hughes, Proc. Phys. Soc. (London) **87,** 535 (1966).
[94] Ionic radii are given by S. Koritnig, in *Landolt-Börnstein Zahlenwerte und Funktionen*, J. Bartels *et al.*, Eds. (Springer-Verlag, Berlin, 1955), Vol. I, Pt. 4.
[95] K. Nassau, Phys. Chem. Solids **24,** 1510 (1963).
[96] B. S. Gourary and F. J. Adrian, Solid State Phys. **10,** 127 (1960).
[97] (a) W. C. Holton and H. Blum, Phys. Rev. **125,** 89 (1962); (b) A. F. Kip, C. Kittel, R. Levy, and A. M. Portis, Phys. Rev. **91,** 1066 (1953); (c) H. C. Wolf and K. H. Hausser, Naturwiss. **46,** 646 (1959); (d) F. Hughes and J. G. Allard, Phys. Rev. **125,** 173 (1962).
[98] E. Jahnke and F. Emde, *Tables of Functions* (Dover Publications, New York, 1945).
[99] M. Abramowitz and I. A. Stegun, *Handbook of Mathematical Tables* (Dover Publications, New York; 1965).
[100] F. H. Horn, Phys. Rev. **97,** 1521 (1954).
[101] J. C. Kemp and V. I. Neeley, Phys. Rev. **132,** 215 (1963).
[102] H. Peisl, R. Balzer and W. Waidelich, Phys. Rev. Letters **17,** 1128 (1966).
[103] K. Thommen, Z. Physik **186,** 347 (1965).
[104] G. A. Andreev and S. F. Bureiko, Fiz. Tverd. Tela **9,** 79 (1967) [Sov. Phys.—Solid State **9,** 58 (1967)].
[105] Y. Fukai, J. Phys. Soc. (Japan) **18,** 1413 (1963); J. E. Nickels, M. A. Fineman, and W. E. Wallace, J. Phys. Chem. **53** 625 (1959).
[106] J. D. Eshelby (private communication).